Influence of Angular Velocity of Pedaling on the Accuracy of the Measurement of Cyclist Power

Abstract

Almost all cycling power meters currently available on the market are positioned on rotating parts of the bicycle (pedals, crank arms, spider, bottom bracket/hub) and, regardless of technical and construction differences, all calculate power on the basis of two physical quantities: torque and angular velocity (or rotational speed – cadence). Both these measures vary during the 360 degrees of each revolution.

The torque / force value is usually measured many times during each rotation, while the angular velocity variation is commonly neglected, considering only its average value for each revolution (cadence).

This, however, introduces an **unpredictable error** into the power calculation. To use the average value of angular velocity means to consider each pedal revolution as perfectly smooth and uniform: but this type of pedal revolution does not exist in reality. Angular velocity may vary due to a number of factors: style of pedaling and physical condition of the cyclist, cadence and effort, slope of the ground, type of chainring used (round or oval), etc. In addition to this, when using an indoor trainer, the angular velocity variation also depends on the inertia it generates, so it may vary significantly from model to model.

Favero Electronics, to ensure the maximum accuracy of its power meters in **all pedaling conditions**, decided to research to what extent the variation of angular velocity during a rotation affects the power calculation.

The study was made with the collaboration of 5 cyclists, who in the past year covered a distance of between 10,000 km and 20,000 km, and whose physical characteristics and athletic preparation are representative of a wide range of power meter users. Each cyclist performed 24 tests, in different situations, both on the road and on indoor trainers.

The results show that variation of angular velocity within a rotation has a considerable impact on the error in calculation of any algorithm that does not take it into account. The miscalculation can be as high as **-1.6% using round chainrings** and **+4.5% using oval chainrings**. Different patterns were also observed depending on the type of indoor trainer used.

The miscalculation may be—even significantly—greater than we found in our study, for the following reasons:

- the test was limited to only 5 cyclists: there is no doubt other cyclists may have styles of pedaling with greater variations of angular velocity;
- only 2 indoor trainer models were considered: other models may produce greater errors;
- slopes greater than 5% (the only value tested) may lead to less uniform rotations and consequently greater errors.

It should be noted that the error observed in this analysis occurs because to measure power the power meter considers the average angular velocity of each rotation. In power meters that use this type of calculation, this error must therefore be added to the accuracy stated by the manufacturer.

The power meter is often used by cyclists to evaluate their improvement over long periods of time and therefore its accuracy is important and should not be influenced by factors that change over time, such as pedaling style (which can also vary with cadence, effort, and physical condition), the type of indoor trainer or chainring used, etc.

This study is part of a wider research that has led **Favero Electronics** to implement the new Assioma **IAV Power** system, which combines proprietary software solutions that take full advantage of the integrated three-axis gyroscope with power calculation algorithms capable of handling the real angular velocity variation during each pedal stroke. The overall accuracy of Assioma has been improved to +/-1% and is ensured in **all pedaling conditions**, regardless of style, type of chainring used (round or oval), type of trainer, etc.

With the new **IAV Power** system, once again **Favero Electronics** marks a major step forward in the field of sports electronics, by using a gyroscope to detect instant angular velocity in cycling power meters, a solution that we believe will become a future technological standard for all power meters placed on rotating parts.

Introduction

In the past few years, demand for cycling power meters has grown considerably, both in the technical and professional field, and among competitive cyclists. At the same time, a demand for accuracy in the measurement of the power the cyclist applies while pedaling has grown. How the signals required to measure power are acquired, therefore, becomes important, just as the subsequent processing of numbers that yields the final result.

On the market today, power meters positioned on rotating parts can be classified into two groups: meters using the average rotational speed within a pedal stroke for the calculation, and those which take its variations into account.

To use the average value of angular velocity means to consider each pedal revolution as perfectly smooth and uniform: this type of pedal revolution does not exist in reality.

Favero Electronics, on a quest to constantly improve the quality of its products, decided to research how much the two different calculation methods influence the accuracy of the final result in different cycling conditions.

Mathematical model

Force F_A applied by the cyclist to the pedal is never fully exploited, since only its F_T part tangential to the rotation of the crank arm produces the moment of force M and is therefore effective in moving the bicycle; the centrifugal component F_C of the applied force is lost for the purposes of movement. The moment of force M is greater the longer the b_C length of the crank arm:

$$M = F_T \cdot b_C$$

The useful power applied by the cyclist to the propelling mechanism depends, other than on the torque, on crank arm rotational speed ω (tied to the cadence):

$$P = M \cdot \omega = F_T \cdot b_C \cdot \omega$$

This power, known as instantaneous power, varies along the 360° of a pedal revolution, since both tangential force F_T, and rotational speed ω vary; normally, to make the measured data available, the average power P_M of an entire pedal revolution cycle is considered. The quantities examined, F_T and ω, are acquired with suitable sensors, at regular intervals that are sufficiently small compared to the total duration of a pedal revolution; the recorded values are called samples.

We shall now examine the two algorithms currently used by commercially available power meters to calculate power, we shall define them as:

- **AAVpwr** algorithm – Average Angular Velocity Power;
- **IAVpwr** algorithm – Istantaneous Angular Velocity Power.

It should be noted that all the following considerations, although referring to the pedal, remain valid even when the points at which the moment of force M and the rotational speed ω are detected are situated on the crank arm or spider or on the bottom bracket/hub.

AAVpwr (Average Angular Velocity Power) **Algorithm**

To calculate the average power P_{M1} of a complete rotation, this method measures the average rotational speed ω_M of the entire pedal stroke and the average tangential force F_{TM}; a final calculation is then carried out:

$$P_{M1} = F_{TM} \cdot b_C \cdot \omega_M$$

To calculate F_{TM}, the sum of samples $F_T(k)$ of the tangential force, acquired during the entire pedal revolution, is divided by the total number of samples N:

$$F_{TM} = \frac{1}{N} \cdot \sum_{k=1}^{N} F_T(k)$$

Normally the average rotational speed ω_M is derived from the complete duration (period) T of a pedal revolution:

$$\omega_M = \frac{2 \cdot \pi}{T}$$

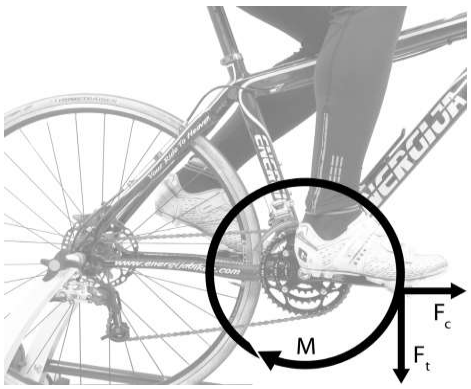

Fig. 1: Forces applied to the pedal. FT: tangential force, FC: centrifugal force, M: moment of force.

IAVpwr (Istantaneous Angular Velocity Power) **Algorithm**

In this second method, to calculate the average power P_{M2} of a complete rotation, the samples of tangential force $F_T(k)$ and rotational speed $\omega(k)$ are acquired together, they are multiplied and the product is progressively summed; at the end of the pedal stroke the result is divided by the number of samples N.

$$P_{M2} = \frac{b_C}{N} \cdot \sum_{k=1}^{N} F_T(k) \cdot \omega(k)$$

This algorithm, therefore, adheres more closely to the instantaneous variations of the tangential force F_T and rotational speed ω within the pedal revolution.

A theoretical description of the power calculation can be found in the appendix.

Test procedure

Tangential force F_T and rotational speed ω were acquired and recorded during the pedal strokes of a number of cyclists, in various cycling conditions. Both power calculation algorithms, AAVpwr and IAVpwr, were then applied to the acquired data(using trapezoidal integration) to compare the results.

Data acquisition and processing

Acquisition of the physical signals, tangential force F_T and rotational speed ω, was performed every 5 ms with an **ASSIOMA®** power meter, with specially designed firmware; this is done in real time and, using the **Bluetooth® low energy technology** radio protocol, the data were transferred to a laptop to be registered in a *csv* file.

Each line of this file has the date, time and instant of sampling, a progressive counter of the radio message to reveal lost packets, and the 24-bit values of the signals mentioned in grams-force [*gf*] and millidegrees per second [*mdps*].

This purposely developed method makes it possible to acquire the signals in the most diverse conditions of use, both in a controlled indoor environment, as well as outdoors.

Since the purpose of the research was not to measure the total power applied by the cyclists, only the signals relevant to the left pedal were acquired; in all subsequent tables, to simulate the power applied by the cyclist with both legs, the power measured by the single pedal was doubled.

The files with the acquired data were then processed offline using the **SCILAB** numerical computation software package to isolate the single pedal strokes and calculate the power using the two algorithms, AAVpwr and IAVpwr.

Materials

The same bicycle was used for all tests with a 172.5 mm crank arms, carrying a pair of **ASSIOMA®** devices equipped with special firmware with the following features:

- internal gyroscope, calibrated with 0.1% accuracy using an encoder and a **National Instruments** NI–6211 and measurement device, to measure the angular velocity;
- eight strain gauges applied to the pedal axle to measure the forces applied to the pedal, with an 0.1% accuracy calibration obtained using M1 precision class calibrated weights; it must be noted that any variations due to temperature act on both algorithms and therefore do not influence the result of their comparison;
- radio communication via **Bluetooth® low energy technology** protocol.

The laptop was provided with an ASUS **USB–BT400** 4.0 USB Bluetooth dongle for radio communication, manufactured by ASUS.

In the lab test setting, the following two indoor trainers, which are representative of the various types of trainers on the market, were used:

- **Qubo** Power Mag, manufactured by Elite;
- **NEO Smart**, manufactured by Tacx.

The following two chainrings were used:

- round: **PRAXIS** 110BCD 50/34 10/11SP 7075–T6;
- oval: **OSYMETRIC** 110mm – 50R.

Cyclist characteristics

Table 1 below reports the general data on each cyclist who performed the complete trial (24 tests); cyclists were selected based on their having covered at least 10,000 km per year and to provide a broad range of possible power meter users.

Table 1: General characteristics of the cyclists undergoing the trial (FTP: functional threshold power).

Cyclist	Sex	Age	Height [cm]	Weight [kg]	FTP [W]	FTP / weight	km / year	type	category
C.01	male	39	172	65	330	5.1	20'000	former pro	2
C.02	male	42	176	71	260	3.7	10'000	competitive cyclist	5
C.03	male	32	180	68	360	5.3	10'000	MTB elite	2
C.04	male	50	170	67	270	4.0	10'000	competitive cyclist	4
C.05	male	19	177	62	280	4.5	20'000	under 23	3

Measurement protocol

The complete trial performed by the **5** cyclists was divided into a set of **24 tests**, in each of which a particular pedaling condition was set to assess its impact on the results of the two algorithms; in particular, the 24 combinations listed in Table 2 were taken into consideration, but there was no mandatory order in which the individual tests needed to be performed.

Before starting the trial, each cyclist warmed up for about 5 minutes, and between each test there was a cool-down phase. Both indoor tests on indoor trainers and outdoor road tests were carried out.

Outdoor road tests

The same itinerary was followed in both directions, shown in Fig. 2, made up of a part on flat terrain (about 7 km) and an uphill slope (about 1 km with a 5% climb) with subsequent descent; the climb was repeated twice, first in a sitting position and then standing on the pedals. The cyclists were asked to remain seated on the flat terrain and to produce a pedaling speed of about 100 rpm on the way out and 90 rpm on the way back. During the uphill parts, besides the position on the bicycle, no other particular indications were given.

The power calculated with the two algorithms was obtained as an average of an interval of at least 90 seconds in which pedaling was uniform; parts with considerable variations where cyclists had stopped, braked, started again, or sprinted were excluded.

Indoor tests on trainers

The cyclists were asked to reach the established pedaling configuration and maintain it for at least 40 seconds while the signals were acquired. The pedaling power calculated using the two algorithms is the average of the entire test duration, identifying the start and end of each pedal stroke.

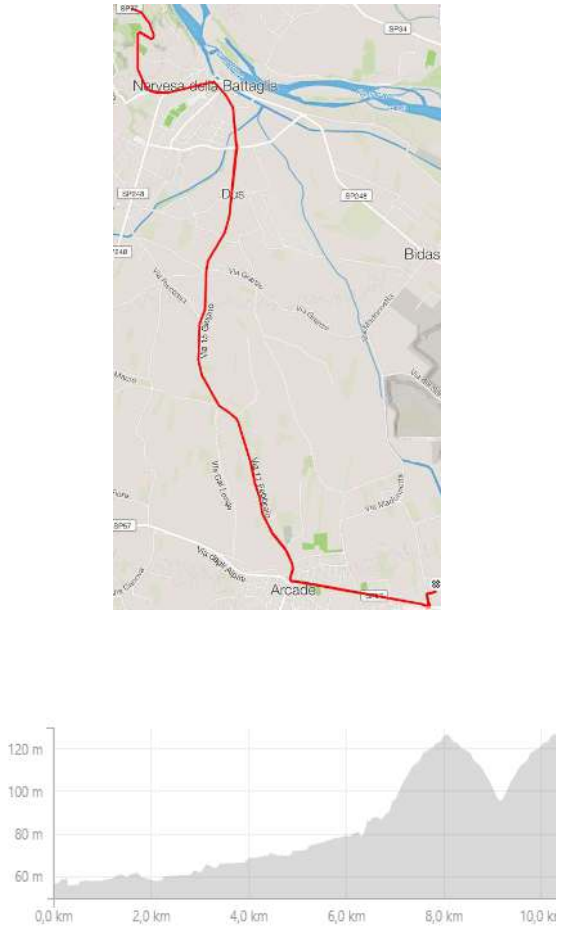

Fig. 2: Road route used in the outdoor test, with elevation data.

Table 2: List and configuration of the tests performed by each cyclist.

Test	chainring	mode	position	FTP [%]	cadence [rpm]
T.1.1.1	round	on Elite Qubo Power Mag trainer	sitting	70	90
T.1.1.2					110
T.1.1.3				95	90
T.1.1.4					70
T.1.2.1	round	on Tacx Neo Smart trainer	sitting	70	90
T.1.2.2					110
T.1.2.3				95	90
T.1.2.4					70
T.1.3.1	round	on the road, flat road	sitting	cyclist's free choice	100
T.1.3.2		on the road, uphill, 5% climb	sitting	cyclist's free choice	Free choice
T.1.3.3		on the road, uphill, 5% climb	standing	cyclist's free choice	Free choice
T.1.3.4		on the road, on flat road	sitting	cyclist's free choice	90
T.2.1.1	oval	on Elite Qubo Power Mag trainer	sitting	70	90
T.2.1.2					110
T.2.1.3				95	90
T.2.1.4					70
T.2.2.1	oval	on Tacx Neo Smart trainer	sitting	70	90
T.2.2.2					110
T.2.2.3				95	90
T.2.2.4					70
T.2.3.1	oval	on the road, flat road	sitting	cyclist's free choice	100
T.2.3.2		on the road, uphill, 5% climb	sitting	cyclist's free choice	Free choice
T.2.3.3		on the road, uphill, 5% climb	standing	cyclist's free choice	Free choice
T.2.3.4		on the road, on flat road	sitting	cyclist's free choice	90

Results

The results of all 24 tests, each performed by 5 cyclists, are reported in the appendix in 24 tables 9 ~ 32.

The results of these tests were grouped by 4 in the following 6 tables 3 ~ 8, each of which refers to a specific test condition.

For each test performed by the 5 cyclists, the average error is recorded, obtained as an average of the 5 cyclists and the maximum error found among the 5 cyclists.

We define error as the percentage difference between the power calculated with the AAVpwr algorithm compared to the one calculated with the IAVpwr algorithm.

It must be borne in mind that AAVpwr erroneously considers the average rotational speed of the entire pedal revolution, while IAVpwr correctly performs the calculation considering its variations.

Test with round ring and Elite Qubo trainer

In the following Table 3 it can be observed that the AAVpwr algorithm, on average, tends to underestimate the power value in the various situations by between −0.22% and −0.86%, but a maximum error of −1.59% is also observed.

Table 3: Results obtained using a round ring and Elite Qubo trainer.

test	description	FTP [%]	cadence [rpm]	average error [%]	maximum error [%]
T.1.1.1	Round ring	70	90	−0.36	−0.71
T.1.1.2	Elite Qubo trainer		110	−0.22	−0.66
T.1.1.3		95	90	−0.51	−1.15
T.1.1.4	Seated		70	−0.86	−1.59

Test with round ring and Tack NEO smart trainer

Even in this situation, the results of which are reported in Table 4, an underestimation error of the power calculated with the AAVpwr algorithm is observed.

Table 4: Results obtained using a round ring and Tacx NEO Smart trainer.

test	description	FTP [%]	cadence [rpm]	average error [%]	maximum error [%]
T.1.2.1	Round ring	70	90	−0.13	−0.22
T.1.2.2	Tacx NEO Smart trainer		110	−0.12	−0.52
T.1.2.3		95	90	−0.17	−0.31
T.1.2.4	Seated		70	−0.30	−0.45

Test with round ring, on the road

In Table 5 an overestimation of power calculated using AAVpwr is evident; the error can reach +0.84%.

Table 5: Results obtained with a round ring, on the road

test	description	average error [%]	maximum error [%]
T.1.3.1	round ring, flat road, seated, 100rpm	+0.04	+0.15
T.1.3.2	round ring, climb 5%, seated	+0.47	+0.63
T.1.3.3	round ring, climb 5%, standing	+0.48	+0.84
T.1.3.4	round ring, flat road, seated, 90rpm	+0.10	+0.20

Test with oval ring and Elite Qubo trainer

With an oval chainring, the overestimation error using AAVpwr is on average +2.5%, with a maximum reaching +3.3%.

Table 6: Results obtained using an oval ring and Elite Qubo trainer.

test	description	FTP [%]	cadence [rpm]	average error [%]	maximum error [%]
T.2.1.1	Oval ring	70	90	+2.73	+2.98
T.2.1.2	Elite Qubo trainer		110	+2.97	+3.30
T.2.1.3		95	90	+2.51	+2.95
T.2.1.4	Seated		70	+1.97	+2.27

Test with oval ring and Tacx NEO Smart trainer

In this situation, the oval ring makes the AAVpwr algorithm overestimate power by an average of +3.1%, peaking at +3.79%.

Table 7: Results using an oval ring and Tacx NEO Smart trainer.

test	description	FTP [%]	cadence [rpm]	average error [%]	maximum error [%]
T.2.2.1	Oval ring	70	90	+3.15	+3.32
T.2.2.2	Tacx NEO Smart trainer		110	+3.21	+3.79
T.2.2.3		95	90	+3.25	+3.76
T.2.2.4	Seated		70	+2.71	+3.14

Test with oval ring, on the road

On the road, the effect of the oval ring on the error resulting from the AAVpwr algorithm is heightened, as it is on average +3.9%, with a maximum of +4.54%.

Table 8: Results obtained with an oval ring, on the road.

test	description	average error [%]	maximum error [%]
T.2.3.1	Oval ring, flat road, seated, 100rpm	+3.85	+4.16
T.2.3.2	Oval ring, climb 5%, seated	+3.90	+4.54
T.2.3.3	Oval ring, climb 5%, standing	+3.93	+4.51
T.2.3.4	Oval ring, flat road, seated, 90rpm	+3.90	+4.29

Discussion

An analysis of the tests and their outcomes leads us to some interesting conclusions; the first conclusion, which is immediately apparent, is the substantial difference of the output of the calculation algorithms depending on whether a round or oval chainring is used.

Below, the results are discussed according to the type of chainring used.

Miscalculations in power using round rings

With the round chainring, the average error made by the AAVpwr algorithm compared to the IAVpwr algorithm varies from −0.86% (test T.1.1.4, Table 3) to +0.48% (test T1.1.3, Table 5), with a maximum value of −1.59%. Observing Table 5, which refers to road tests, the measurement error on flat roads is negligible, (maximum +0.2%), while with a 5% climb there is an average +0.5% overestimation, which is justified by the greater irregularity in pedal strokes under strain. We can assume that by increasing the slope the miscalculation would increase.

Observing, instead, tables 3 and 4, which refer to tests on indoor trainers, an underestimation is evident, which is different for the two types of trainers and can be as high as −1.59% (test T.1.1.4, table 3).

Evaluating the error interval for the same cyclist by looking at all his tests on both road and trainers (see: table 37 of cyclist C.03), the error can be observed to go from −1.59% of test T.1.1.4 to +0.62% of test T.1.3.2, so there is a 2.21% difference. This means that if the power meter uses the AAVpwr algorithm, it can show the same power even though there is actually a 2.21% difference.

Miscalculations in power using oval rings

We would like to point out that the oval ring used (OSYMETRIC 110mm – 50R) is one of the most ovalized currently on the market, therefore less ovalized chainrings would cause lower errors.

The AAVpwr algorithm, which does not take into account the rotational speed during the pedal revolution, overestimates power by an average of about 2 ~ 4 % (Tables 6, 7 and 8) reaching a maximum error of +4.54%. The overestimation is observed especially on the road tests, compared to tests on trainers (about 1% more), and a difference in the response of the trainers themselves is also observed (Tables 6 and 7).

It must be noticed that this study does not set out to find the reasons for the different behavior observed on the road vs. on trainers and on one trainer vs. the other—a difference which is presumably due to a different inertia behavior and braking method on the trainers—but only to ascertain their difference.

Analyzing, even in this case, the error interval for the same cyclist by looking at all his road and trainer tests (see: table 34 of cyclist C.01), the error goes from +1.85% of test T.2.1.4 to +4.51% of test T.2.3.3, with a difference as great as 2.65%. This means that if the power meter uses the AAVPwr algorithm, it can show the same power output even though there is actually a 2.65% difference.

General observations

Since our study only considered a limited number of situations, and, above all, the trials were performed by only 5 cyclists and only 2 trainers were used, it can be assumed that if we were to widen the case study, the error could only increase.

Even with climbs steeper than 5% the error might increase.

In all cases considered, both those with a round ring and those with an oval ring, in addition to the identified errors, one needs to add the accuracy stated by the manufacturer of power meters that do not consider in the calculation the variation in rotational speed, an error which is generally around 1%.

To what extent the percentage error of the AAVpwr algorithm depends on the percentage variation of the pedaling rotational speed (maximum − minimum, compared to average) is shown in the chart of Fig. 3, which also shows a 4th-degree polynomial trend line, with a high correlation coefficient $R^2 = 0.93$. This chart shows the results of all the tests divided by cyclist, while the trend line refers to all of them. It is evident that all cycling conditions that produce an increase in the unevenness of rotational speed within the pedal stroke progressively influence the error in the calculation of power; these conditions depend on the equipment used (chainrings), cycling situation (on trainer or road, flat road or climb), as well as the pedaling style of each cyclist.

> It is worth pointing out that all the errors detected so far, which occur when the variation in speed within the pedal rotation cycle is not taken into account in calculating the power, are exactly the same for all power meters installed on pedals, crank arms, crank spiders/chainring, and bottom bracket/hub, since they are all subject to the same variations in speed.

This study proves the importance of equipping power meters with a gyroscope to enable them to precisely detect the instantaneous angular velocity.

Since the IAVpwr algorithm correctly measures power regardless of whether a round or an oval chainring is used, a power meter which uses the IAVpwr algorithm may help cyclists assess the type of chainring that allows them to express greater power.

Acknowledgments

We would like to thank the cyclists who participated in the tests for their collaboration and the considerable effort they made.

References

1. www.scilab.org
2. www.elite−it.com
3. www.tacx.com
4. www.thisisant.com
5. www.bluetooth.com

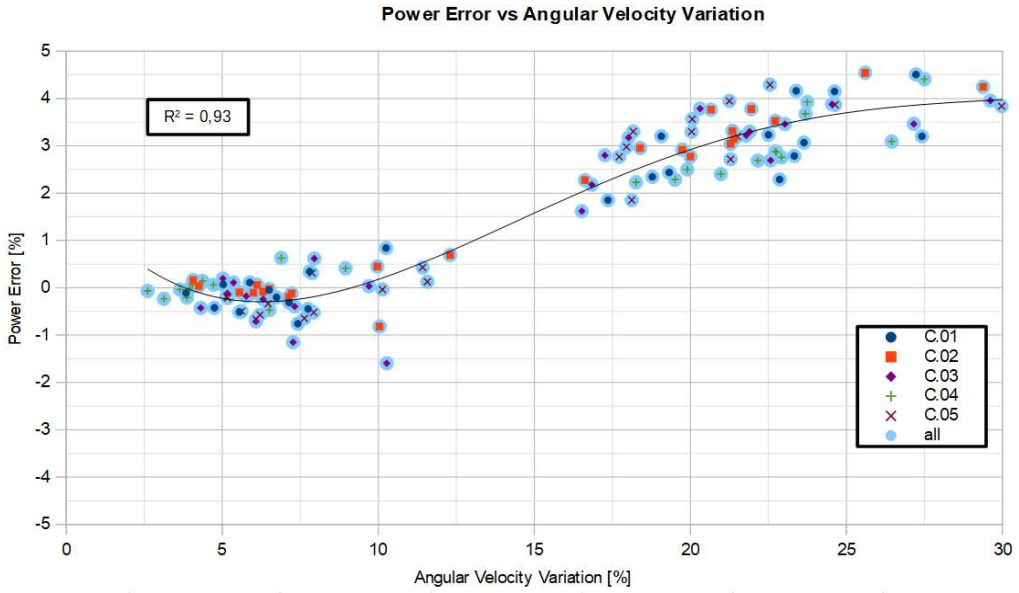

Fig. 3: Correlation between the variation of angular velocity and error of the AAVpwr algorithm in the power calculation.

Results by test type

In this section, the results of the 24 tests are reported 24 tables, from 9 to 32. The rows show: **(a)** the cyclist identification code, **(b)** the *csv* file produced during the test, **(c)** the maximum–minimum rotational speed variation in a pedal revolution compared to the average speed, **(d)** the power calculated with the IAVpwr algorithm, **(e)** the power calculated with the AAVpwr algorithm, **(f)** the percentage error resulting from the latter algorithm.

The power values shown are the values obtained from the left pedal only, multiplied by two. To calculate the torque, a 172.5 mm crank arm length was used. Each table is connected to a chart showing a cyclist's typical pedal stroke.

Table 9: Test **T.1.1.1** – round ring, Elite Qubo trainer, seated, FTP 70%, cadence 90 rpm (chart T.1.1.1 – A01.png)

cyclist	file	angular velocity variation [%]	IAVpwr [W]	AAVpwr [W]	power error [%]	
C.01	T.1.1.1 – C01 – 01 (2018.02.05 10.03.27).csv	4.8	258.5	257.4	−0.42	max = −0.71 med = −0.36
C.02	T.1.1.1 – C02 – 01 (2018.02.09 11.33.13).csv	4.3	180.6	180.7	+0.04	
C.03	T.1.1.1 – C03 – 01 (2018.02.15 03.46.22).csv	6.1	261.3	259.4	−0.71	
C.04	T.1.1.1 – C04 – 01 (2018.02.16 03.54.31).csv	3.1	216.1	215.6	−0.23	
C.05	T.1.1.1 – C05 – 01 (2018.02.19 03.31.24).csv	5.6	234.8	233.7	−0.49	

Table 10: Test **T.1.1.2** – round ring, Elite Qubo trainer, seated, FTP 70%, cadence 110 rpm (chart T.1.1.2 – A01.png)

cyclist	file	angular velocity variation [%]	IAVpwr [W]	AAVpwr [W]	power error [%]	
C.01	T.1.1.2 – C01 – 01 (2018.02.05 10.05.04).csv	3.8	225.6	225.4	−0.11	
C.02	T.1.1.2 – C02 – 01 (2018.02.09 11.34.39).csv	4.1	188.7	189.0	+0.16	
C.03	T.1.1.2 – C03 – 01 (2018.02.15 03.48.03).csv	4.3	256.2	255.1	−0.43	max = −0.43 med = −0.22
C.04	T.1.1.2 – C04 – 01 (2018.02.16 03.56.33).csv	2.6	172.8	172.7	−0.06	
C.05	T.1.1.2 – C05 – 01 (2018.02.19 03.33.06).csv	6.1	222.6	221.1	−0.66	

Table 11: Test **T.1.1.3** – round ring, Elite Qubo trainer, seated, FTP 95%, cadence 90 rpm (chart T.1.1.3 – A01.png)

cyclist	file	angular velocity variation [%]	IAVpwr [W]	AAVpwr [W]	power error [%]	
C.01	T.1.1.3 – C01 – 01 (2018.02.05 10.06.35).csv	5.6	306.8	305.3	−0.51	
C.02	T.1.1.3 – C02 – 01 (2018.02.09 11.36.31).csv	5.6	264.1	263.8	−0.09	
C.03	T.1.1.3 – C03 – 01 (2018.02.15 03.50.03).csv	7.3	326.3	322.6	−1.15	max = −1.15 med = −0.51
C.04	T.1.1.3 – C04 – 01 (2018.02.16 03.58.53).csv	3.9	276.6	276.0	−0.21	
C.05	T.1.1.3 – C05 – 01 (2018.02.19 03.35.16).csv	6.2	262.7	261.2	−0.57	

Table 12: Test **T.1.1.4** – round ring, Elite Qubo trainer, seated, FTP 95%, cadence 70 rpm (chart T.1.1.4 – A01.png)

cyclist	file	angular velocity variation [%]	IAVpwr [W]	AAVpwr [W]	power error [%]	
C.01	T.1.1.4 – C01 – 01 (2018.02.05 10.09.40).csv	7.4	286.0	283.8	−0.76	
C.02	T.1.1.4 – C02 – 01 (2018.02.09 11.39.26).csv	10.0	234.1	232.1	−0.82	
C.03	T.1.1.4 – C03 – 01 (2018.02.15 03.52.03).csv	10.3	335.4	330.0	−1.59	max = −1.59 med = −0.86
C.04	T.1.1.4 – C04 – 01 (2018.02.16 04.01.28).csv	6.5	261.1	259.9	−0.47	
C.05	T.1.1.4 – C05 – 01 (2018.02.19 03.37.31).csv	7.6	234.1	232.6	−0.64	

Table 13: Test **T.1.2.1** – round ring, Tacx NEO Smart trainer, seated, FTP 70%, cadence 90 rpm (chart T.1.2.1 – A01.png)

cyclist	file	angular velocity variation [%]	IAVpwr [W]	AAVpwr [W]	power error [%]	
C.01	T.1.2.1 – C01 – 01 (2018.02.05 10.14.09).csv	6.7	227.3	226.8	−0.20	max = −0.22 med = −0.13
C.02	T.1.2.1 – C02 – 01 (2018.02.09 11.44.28).csv	6.3	186.2	186.0	−0.08	
C.03	T.1.2.1 – C03 – 01 (2018.02.15 03.57.01).csv	5.2	258.0	257.7	−0.12	
C.04	T.1.2.1 – C04 – 01 (2018.02.16 04.06.48).csv	3.7	200.5	200.4	−0.04	
C.05	T.1.2.1 – C05 – 01 (2018.02.19 03.43.16).csv	5.2	224.2	223.7	−0.22	

Table 14: Test **T.1.2.2** – round ring, Tacx NEO Smart trainer, seated, FTP 70%, cadence 110 rpm (chart T.1.2.2 – A01.png)

cyclist	file	angular velocity variation [%]	IAVpwr [W]	AAVpwr [W]	power error [%]	
C.01	T.1.2.2 – C01 – 01 (2018.02.05 10.15.39).csv	6.5	247.2	247.1	−0.05	max = −0.52 med = −0.12
C.02	T.1.2.2 – C02 – 01 (2018.02.09 11.46.03).csv	6.1	206.4	206.5	+0.06	
C.03	T.1.2.2 – C03 – 01 (2018.02.15 03.58.58).csv	5.8	273.5	273.0	−0.18	
C.04	T.1.2.2 – C04 – 01 (2018.02.16 04.09.10).csv	4.0	209.9	210.1	+0.07	
C.05	T.1.2.2 – C05 – 01 (2018.02.19 03.45.09).csv	7.9	250.1	248.8	−0.52	

Table 15: Test **T.1.2.3** – round ring, Tacx NEO Smart trainer, seated, FTP 95%, cadence 90 rpm (chart T.1.2.3 – A01.png)

cyclist	file	angular velocity variation [%]	IAVpwr [W]	AAVpwr [W]	power error [%]	
C.01	T.1.2.3 – C01 – 01 (2018.02.05 10.17.51).csv	7.1	310.7	309.7	−0.31	
C.02	T.1.2.3 – C02 – 01 (2018.02.09 11.48.28).csv	7.2	231.8	231.6	−0.12	
C.03	T.1.2.3 – C03 – 01 (2018.02.15 04.00.38).csv	6.3	333.4	332.6	−0.24	max = −0.31 med = −0.17
C.04	T.1.2.3 – C04 – 01 (2018.02.16 04.11.35).csv	4.0	252.7	252.7	−0.01	
C.05	T.1.2.3 – C05 – 01 (2018.02.19 03.47.08).csv	5.1	274.1	273.6	−0.19	

Table 16: Test **T.1.2.4** – round ring, Tacx NEO Smart trainer, seated, FTP 95%, cadence 70 rpm (chart T.1.2.4 – A01.png)

cyclist	file	angular velocity variation [%]	IAVpwr [W]	AAVpwr [W]	power error [%]	
C.01	T.1.2.4 – C01 – 01 (2018.02.05 10.19.52).csv	7.8	304.2	302.8	−0.45	
C.02	T.1.2.4 – C02 – 01 (2018.02.09 11.50.29).csv	7.1	228.6	228.2	−0.20	
C.03	T.1.2.4 – C03 – 01 (2018.02.15 04.03.04).csv	7.3	330.8	329.5	−0.39	max = −0.45 med = −0.30
C.04	T.1.2.4 – C04 – 01 (2018.02.16 04.13.47).csv	5.2	243.2	242.9	−0.13	
C.05	T.1.2.4 – C05 – 01 (2018.02.19 03.49.14).csv	6.5	272.8	271.9	−0.33	

Table 17: Test **T.1.3.1** – round ring, on flat road, seated, cadence 100 rpm (chart T.1.3.1 – A01.png)

cyclist	file	angular velocity variation [%]	IAVpwr [W]	AAVpwr [W]	power error [%]	
C.01	T.1.3.1 – C01 – 01 (2018.02.05 10.46.08).csv	5.0	205.8	205.9	+0.07	
C.02	T.1.3.1 – C02 – 01 (2018.02.09 10.44.12).csv	6.0	161.3	161.2	−0.10	
C.03	T.1.3.1 – C03 – 01 (2018.02.15 02.45.51).csv	5.4	245.7	246.0	+0.11	max = +0.15 med = +0.04
C.04	T.1.3.1 – C04 – 01 (2018.02.16 02.55.38).csv	4.4	168.8	169.0	+0.15	
C.05	T.1.3.1 – C05 – 01 (2018.02.19 02.38.43).csv	10.1	178.8	178.8	−0.04	

Table 18: Test **T.1.3.2** – round ring, on the road, 5% climb, seated (chart T.1.3.2 – A01.png)

cyclist	file	angular velocity variation [%]	IAVpwr [W]	AAVpwr [W]	power error [%]	
C.01	T.1.3.2 – C01 – 01 (2018.02.05 11.02.14).csv	7.8	331.4	332.5	+0.34	max = +0.63 med = +0.47
C.02	T.1.3.2 – C02 – 01 (2018.02.09 11.01.29).csv	10.0	268.9	270.1	+0.45	
C.03	T.1.3.2 – C03 – 01 (2018.02.15 03.05.54).csv	8.0	357.2	359.4	+0.62	
C.04	T.1.3.2 – C04 – 01 (2018.02.16 03.11.41).csv	6.9	258.8	260.4	+0.63	
C.05	T.1.3.2 – C05 – 01 (2018.02.19 02.54.32).csv	7.9	259.5	260.3	+0.31	

Table 19: Test **T.1.3.3** – round ring, on the road, 5% climb, standing (chart T.1.3.3 – A01.png)

cyclist	file	angular velocity variation [%]	IAVpwr [W]	AAVpwr [W]	power error [%]	
C.01	T.1.3.3 – C01 – 01 (2018.02.05 11.02.14).csv	10.3	350.9	353.8	+0.84	max = +0.84 med = +0.48
C.02	T.1.3.3 – C02 – 01 (2018.02.09 11.06.37).csv	12.3	286.7	288.7	+0.69	
C.03	T.1.3.3 – C03 – 01 (2018.02.15 03.15.11).csv	9.7	360.6	360.7	+0.03	
C.04	T.1.3.3 – C04 – 01 (2018.02.16 03.17.11).csv	9.0	306.0	307.3	+0.41	
C.05	T.1.3.3 – C05 – 01 (2018.02.19 03.00.28).csv	11.4	292.2	293.5	+0.43	

Table 20: Test **T.1.3.4** – round ring, on the road, flat road, seated, cadence 90rpm (chart T.1.3.4 – A01.png)

cyclist	file	angular velocity variation [%]	IAVpwr [W]	AAVpwr [W]	power error [%]	
C.01	T.1.3.4 – C01 – 01 (2018.02.05 11.11.14).csv	5.9	241.6	241.9	+0.11	
C.02	T.1.3.4 – C02 – 01 (2018.02.09 11.11.38).csv	6.5	215.1	215.1	−0.02	
C.03	T.1.3.4 – C03 – 01 (2018.02.15 03.20.22).csv	5.0	262.1	262.6	+0.20	max = +0.20 med = +0.10
C.04	T.1.3.4 – C04 – 01 (2018.02.16 03.22.57).csv	4.7	165.8	165.9	+0.06	
C.05	T.1.3.4 – C05 – 01 (2018.02.19 03.06.14).csv	11.6	179.9	180.1	+0.13	

Table 21: Test **T.2.1.1** – oval ring, Elite Qubo trainer, seated, FTP 70%, cadence 90 rpm (chart T.2.1.1 – A01.png)

cyclist	file	angular velocity variation [%]	IAVpwr [W]	AAVpwr [W]	power error [%]	
C.01	T.2.1.1 – C01 – 01 (2018.02.05 09.50.29).csv	19.3	251.4	257.5	+2.44	
C.02	T.2.1.1 – C02 – 01 (2018.02.09 12.06.38).csv	19.7	180.7	186.0	+2.92	
C.03	T.2.1.1 – C03 – 01 (2018.02.15 04.21.03).csv	17.3	270.3	277.9	+2.80	max = +2.98 med = +2.73
C.04	T.2.1.1 – C04 – 01 (2018.02.16 04.31.26).csv	19.9	213.5	218.8	+2.50	
C.05	T.2.1.1 – C05 – 01 (2018.02.19 04.08.29).csv	18.0	221.4	228.0	+2.98	

Table 22: Test **T.2.1.2** – oval ring, Elite Qubo trainer, seated, FTP 70%, cadence 110 rpm (chart T.2.1.2 – A01.png)

cyclist	file	angular velocity variation [%]	IAVpwr [W]	AAVpwr [W]	power error [%]	
C.01	T.2.1.2 – C01 – 01 (2018.02.05 09.51.57).csv	19.1	227.3	234.6	+3.20	
C.02	T.2.1.2 – C02 – 01 (2018.02.09 12.07.59).csv	20.0	193.7	199.1	+2.77	
C.03	T.2.1.2 – C03 – 01 (2018.02.15 04.24.02).csv	18.0	260.3	268.5	+3.17	max = +3.30 med = +2.97
C.04	T.2.1.2 – C04 – 01 (2018.02.16 04.33.38).csv	21.0	195.3	200.0	+2.40	
C.05	T.2.1.2 – C05 – 01 (2018.02.19 04.10.12).csv	18.2	187.8	194.0	+3.30	

Table 23: Test **T.2.1.3** – oval ring, Elite Qubo trainer, seated, FTP 95%, cadence 90 rpm (chart T.2.1.3 – A01.png)

cyclist	file	angular velocity variation [%]	IAVpwr [W]	AAVpwr [W]	power error [%]	
C.01	T.2.1.3 – C01 – 01 (2018.02.05 09.53.59).csv	18.8	325.1	332.7	+2.34	max = +2.95 med = +2.51
C.02	T.2.1.3 – C02 – 01 (2018.02.09 12.10.26).csv	18.4	226.1	232.7	+2.95	
C.03	T.2.1.3 – C03 – 01 (2018.02.15 04.25.44).csv	16.8	340.9	348.3	+2.18	
C.04	T.2.1.3 – C04 – 01 (2018.02.16 04.35.20).csv	19.5	291.4	298.0	+2.29	
C.05	T.2.1.3 – C05 – 01 (2018.02.19 04.12.56).csv	17.7	280.6	288.4	+2.77	

Table 24: Test **T.2.1.4** – oval ring, Elite Qubo trainer, seated, FTP 95%, cadence 70 rpm (chart T.2.1.4 – A01.png)

cyclist	file	angular velocity variation [%]	IAVpwr [W]	AAVpwr [W]	power error [%]	
C.01	T.2.1.4 – C01 – 01 (2018.02.05 09.55.59).csv	17.4	309.0	314.8	+1.85	max = +2.27 med = +1.96
C.02	T.2.1.4 – C02 – 01 (2018.02.09 12.12.00).csv	16.6	235.8	241.2	+2.27	
C.03	T.2.1.4 – C03 – 01 (2018.02.15 04.29.55).csv	16.5	312.6	317.7	+1.62	
C.04	T.2.1.4 – C04 – 01 (2018.02.16 04.37.22).csv	18.3	278.4	284.6	+2.23	
C.05	T.2.1.4 – C05 – 01 (2018.02.19 04.15.42).csv	18.1	258.5	263.3	+1.85	

Table 25: Test **T.2.2.1** – oval ring, Tacx NEO Smart trainer, seated, FTP 70%, cadence 90 rpm (chart T.2.2.1 – A01.png)

cyclist	file	angular velocity variation [%]	IAVpwr [W]	AAVpwr [W]	power error [%]	
C.01	T.2.2.1 – C01 – 01 (2018.02.05 09.25.05).csv	23.6	224.2	231.1	+3.07	
C.02	T.2.2.1 – C02 – 01 (2018.02.09 11.56.05).csv	21.4	193.8	200.2	+3.32	
C.03	T.2.2.1 – C03 – 01 (2018.02.15 04.09.36).csv	21.9	257.6	266.1	+3.30	max = +3.32 med = +3.15
C.04	T.2.2.1 – C04 – 01 (2018.02.16 04.19.53).csv	22.7	202.6	208.4	+2.88	
C.05	T.2.2.1 – C05 – 01 (2018.02.19 03.55.25).csv	21.5	221.9	229.0	+3.20	

Table 26: Test **T.2.2.2** – oval ring, Tacx NEO Smart trainer, seated, FTP 70%, cadence 110 rpm (chart T.2.2.2 – A01.png)

cyclist	file	angular velocity variation [%]	IAVpwr [W]	AAVpwr [W]	power error [%]	
C.01	T.2.2.2 – C01 – 01 (2018.02.05 09.34.20).csv	23.3	267.7	275.2	+2.79	
C.02	T.2.2.2 – C02 – 01 (2018.02.09 11.57.52).csv	21.3	208.6	214.9	+3.04	
C.03	T.2.2.2 – C03 – 01 (2018.02.15 04.11.04).csv	20.3	268.6	278.8	+3.79	max = +3.79 med = +3.21
C.04	T.2.2.2 – C04 – 01 (2018.02.16 04.22.07).csv	22.8	214.5	220.6	+2.86	
C.05	T.2.2.2 – C05 – 01 (2018.02.19 03.57.13).csv	20.1	244.4	253.1	+3.56	

Table 27: Test **T.2.2.3** – oval ring, Tacx NEO Smart trainer, seated, FTP 95%, cadence 90 rpm (chart T.2.2.3 – A01.png)

cyclist	file	angular velocity variation [%]	IAVpwr [W]	AAVpwr [W]	power error [%]	
C.01	T.2.2.3 – C01 – 01 (2018.02.05 09.38.42).csv	22.5	230.6	238.0	+3.23	
C.02	T.2.2.3 – C02 – 01 (2018.02.09 12.00.23).csv	20.7	234.5	243.3	+3.76	
C.03	T.2.2.3 – C03 – 01 (2018.02.15 04.13.10).csv	21.8	329.5	340.1	+3.22	max = +3.76 med = +3.25
C.04	T.2.2.3 – C03 – 01 (2018.02.16 04.24.24).csv	22.9	258.2	265.4	+2.76	
C.05	T.2.2.3 – C05 – 01 (2018.02.19 04.00.10).csv	20.0	272.7	281.7	+3.30	

Table 28: Test **T.2.2.4** – oval ring, Tacx NEO Smart trainer, seated, FTP 95%, cadence 70 rpm (chart T.2.2.4 – A01.png)

cyclist	file	angular velocity variation [%]	IAVpwr [W]	AAVpwr [W]	power error [%]	
C.01	T.2.2.4 – C01 – 01 (2018.02.05 09.45.31).csv	22.9	306.7	313.7	+2.29	max = +3.14 med = +2.71
C.02	T.2.2.4 – C02 – 01 (2018.02.09 12.02.29).csv	21.4	226.2	233.3	+3.14	
C.03	T.2.2.4 – C03 – 01 (2018.02.15 04.15.27).csv	22.6	333.1	342.1	+2.69	
C.04	T.2.2.4 – C04 – 01 (2018.02.16 04.26.43).csv	22.2	247.3	253.9	+2.69	
C.05	T.2.2.4 – C05 – 01 (2018.02.19 04.02.24).csv	21.3	268.2	275.5	+2.72	

Table 29: Test **T.2.3.1** – oval ring, on the road, flat road, seated, cadence 100 rpm (chart T.2.3.1 – A01.png)

cyclist	file	angular velocity variation [%]	IAVpwr [W]	AAVpwr [W]	power error [%]	
C.01	T.2.3.1 – C01 – 01 (2018.02.05 11.28.00).csv	23.4	209.5	218.2	+4.16	max = +4.16 med = +3.86
C.02	T.2.3.1 – C02 – 01 (2018.02.09 09.44.07).csv	22.0	160.7	166.7	+3.78	
C.03	T.2.3.1 – C03 – 01 (2018.02.15 01.57.39).csv	23.0	257.7	266.6	+3.46	
C.04	T.2.3.1 – C04 – 01 (2018.02.16 02.07.33).csv	23.8	180.2	187.3	+3.93	
C.05	T.2.3.1 – C05 – 01 (2018.02.19 01.46.54).csv	21.3	191.3	198.8	+3.95	

Table 30: Test **T.2.3.2** – oval ring , on the road, 5% climb, seated (chart T.2.3.2 – A01.png)

cyclist	file	angular velocity variation [%]	IAVpwr [W]	AAVpwr [W]	power error [%]	
C.01	T.2.3.2 – C01 – 02 (2018.02.05 11.43.40).csv	27.4	325.9	336.4	+3.20	
C.02	T.2.3.2 – C02 – 01 (2018.02.09 10.12.57).csv	25.6	255.0	266.6	+4.54	
C.03	T.2.3.2 – C03 – 01 (2018.02.15 02.12.10).csv	27.2	350.2	362.3	+3.46	max = +4.54 med = +3.90
C.04	T.2.3.2 – C04 – 01 (2018.02.16 02.23.41).csv	27.5	275.0	287.1	+4.41	
C.05	T.2.3.2 – C05 – 01 (2018.02.19 02.09.44).csv	24.6	263.5	273.6	+3.87	

Table 31: Test **T.2.3.3** – oval ring, on the road, 5% climb, standing (chart T.2.3.3 – A01.png)

cyclist	file	angular velocity variation [%]	IAVpwr [W]	AAVpwr [W]	power error [%]	
C.01	T.2.3.3 – C01 – 01 (2018.02.05 11.47.45).csv	27.2	349.1	364.9	+4.51	
C.02	T.2.3.3 – C02 – 01 (2018.02.09 10.18.13).csv	29.4	303.3	316.2	+4.25	
C.03	T.2.3.3 – C03 – 01 (2018.02.15 02.23.30).csv	29.6	383.3	398.5	+3.96	max = +4.51 med = +3.93
C.04	T.2.3.3 – C01 – 01 (2018.02.16 02.29.29).csv	26.5	308.5	318.0	+3.09	
C.05	T.2.3.3 – C05 – 01 (2018.02.19 02.15.59).csv	30.0	310.5	322.4	+3.84	

Table 32: Test **T.2.3.4** – oval ring, on the road, flat road, seated, cadence 90 rpm (chart T.2.3.4 – A01.png)

cyclist	file	angular velocity variation [%]	IAVpwr [W]	AAVpwr [W]	power error [%]	
C.01	T.2.3.4 – C01 – 01 (2018.02.05 11.52.20).csv	24.6	222.6	231.9	+4.15	
C.02	T.2.3.4 – C02 – 01 (2018.02.09 10.23.07).csv	22.7	232.4	240.6	+3.53	
C.03	T.2.3.4 – C03 – 01 (2018.02.15 02.28.33).csv	24.5	276.5	287.3	+3.88	max = +4.29 med = +3.91
C.04	T.2.3.4 – C04 – 01 (2018.02.16 02.34.49).csv	23.7	159.7	165.6	+3.68	
C.05	T.2.3.4 – C05 – 01 (2018.02.19 02.21.44).csv	22.6	178.1	185.8	+4.29	

Results divided by cyclist

The following test results refer to the individual cyclists. The columns of the following table report: **(a)** the test's identification code, **(b)** the maximum–minimum variation in rotational speed within a pedal stroke compared to the average speed, **(c)** the *csv* file produced during the test, **(d)** the power calculated with the IAVpwr algorithm, **(e)** the power value given by the AAVpwr algorithm, **(f)** the percentage error resulting from the latter algorithm. To calculate the torque, a 172.5 mm crank arm length was used.

The power values shown are the values obtained from the left pedal only, multiplied by two.

Table 33: Cyclist **C.01** – summary of the results of tests using a round ring

test	file	angular velocity variation [%]	IAVpwr [W]	AAVpwr [W]	power error [%]
T.1.1.1	T.1.1.1 – C01 – 01 (2018.02.05 10.03.27).csv	4.8	258.5	257.4	−0.42
T.1.1.2	T.1.1.2 – C01 – 01 (2018.02.05 10.05.04).csv	3.8	225.6	225.4	−0.11
T.1.1.3	T.1.1.3 – C01 – 01 (2018.02.05 10.06.35).csv	5.6	306.8	305.3	−0.51
T.1.1.4	T.1.1.4 – C01 – 01 (2018.02.05 10.09.40).csv	7.4	286.0	283.8	−0.76
T.1.2.1	T.1.2.1 – C01 – 01 (2018.02.05 10.14.09).csv	6.7	227.3	226.8	−0.20
T.1.2.2	T.1.2.2 – C01 – 01 (2018.02.05 10.15.39).csv	6.5	247.2	247.1	−0.05
T.1.2.3	T.1.2.3 – C01 – 01 (2018.02.05 10.17.51).csv	7.1	310.7	309.7	−0.31
T.1.2.4	T.1.2.4 – C01 – 01 (2018.02.05 10.19.52).csv	7.8	304.2	302.8	−0.45
T.1.3.1	T.1.3.1 – C01 – 01 (2018.02.05 10.46.08).csv	5.0	205.8	205.9	+0.07
T.1.3.2	T.1.3.2 – C01 – 01 (2018.02.05 11.02.14).csv	7.8	331.4	332.5	+0.34
T.1.3.3	T.1.3.3 – C01 – 01 (2018.02.05 11.02.14).csv	10.3	350.9	353.8	+0.84
T.1.3.4	T.1.3.4 – C01 – 01 (2018.02.05 11.11.14).csv	5.9	241.6	241.9	+0.11

Table 34: Cyclist **C.01** – summary of the results of tests using an oval ring

test	file	angular velocity variation [%]	IAVpwr [W]	AAVpwr [W]	power error [%]
T.2.1.1	T.2.1.1 – C01 – 01 (2018.02.05 09.50.29).csv	19.3	251.4	257.5	+2.44
T.2.1.2	T.2.1.2 – C01 – 01 (2018.02.05 09.51.57).csv	19.1	227.3	234.6	+3.20
T.2.1.3	T.2.1.3 – C01 – 01 (2018.02.05 09.53.59).csv	18.8	325.1	332.7	+2.34
T.2.1.4	T.2.1.4 – C01 – 01 (2018.02.05 09.55.59).csv	17.4	309.0	314.8	+1.85
T.2.2.1	T.2.2.1 – C01 – 01 (2018.02.05 09.25.05).csv	23.6	224.2	231.1	+3.07
T.2.2.2	T.2.2.2 – C01 – 01 (2018.02.05 09.34.20).csv	23.3	267.7	275.2	+2.79
T.2.2.3	T.2.2.3 – C01 – 01 (2018.02.05 09.38.42).csv	22.5	230.6	238.0	+3.23
T.2.2.4	T.2.2.4 – C01 – 01 (2018.02.05 09.45.31).csv	22.9	306.7	313.7	+2.29
T.2.3.1	T.2.3.1 – C01 – 01 (2018.02.05 11.28.00).csv	23.4	209.5	218.2	+4.16
T.2.3.2	T.2.3.2 – C01 – 02 (2018.02.05 11.43.40).csv	27.4	325.9	336.4	+3.20
T.2.3.3	T.2.3.3 – C01 – 01 (2018.02.05 11.47.45).csv	27.2	349.1	364.9	+4.51
T.2.3.4	T.2.3.4 – C01 – 01 (2018.02.05 11.52.20).csv	24.6	222.6	231.9	+4.15

Table 35: Cyclist **C.02** – summary of the results of tests using a round ring.

test	file	angular velocity variation [%]	IAVpwr [W]	AAVpwr [W]	power error [%]
T.1.1.1	T.1.1.1 – C02 – 01 (2018.02.09 11.33.13).csv	4.3	180.6	180.7	+0.04
T.1.1.2	T.1.1.2 – C02 – 01 (2018.02.09 11.34.39).csv	4.1	188.7	189.0	+0.16
T.1.1.3	T.1.1.3 – C02 – 01 (2018.02.09 11.36.31).csv	5.6	264.1	263.8	−0.09
T.1.1.4	T.1.1.4 – C02 – 01 (2018.02.09 11.39.26).csv	10.0	234.1	232.1	−0.82
T.1.2.1	T.1.2.1 – C02 – 01 (2018.02.09 11.44.28).csv	6.3	186.2	186.0	−0.08
T.1.2.2	T.1.2.2 – C02 – 01 (2018.02.09 11.46.03).csv	6.1	206.4	206.5	+0.06
T.1.2.3	T.1.2.3 – C02 – 01 (2018.02.09 11.48.28).csv	7.2	231.8	231.6	−0.12
T.1.2.4	T.1.2.4 – C02 – 01 (2018.02.09 11.50.29).csv	7.1	228.6	228.2	−0.20
T.1.3.1	T.1.3.1 – C02 – 01 (2018.02.09 10.44.12).csv	6.0	161.3	161.2	−0.10
T.1.3.2	T.1.3.2 – C02 – 01 (2018.02.09 11.01.29).csv	10.0	268.9	270.1	+0.45
T.1.3.3	T.1.3.3 – C02 – 01 (2018.02.09 11.06.37).csv	12.3	286.7	288.7	+0.69
T.1.3.4	T.1.3.4 – C02 – 01 (2018.02.09 11.11.38).csv	6.5	215.1	215.1	−0.02

Table 36: Cyclist **C.02** – summary of the results of tests using an oval ring.

test	file	angular velocity variation [%]	IAVpwr [W]	AAVpwr [W]	power error [%]
T.2.1.1	T.2.1.1 – C02 – 01 (2018.02.09 12.06.38).csv	19.7	180.7	186.0	+2.92
T.2.1.2	T.2.1.2 – C02 – 01 (2018.02.09 12.07.59).csv	20.0	193.7	199.1	+2.77
T.2.1.3	T.2.1.3 – C02 – 01 (2018.02.09 12.10.26).csv	18.4	226.1	232.7	+2.95
T.2.1.4	T.2.1.4 – C02 – 01 (2018.02.09 12.12.00).csv	16.6	235.8	241.2	+2.27
T.2.2.1	T.2.2.1 – C02 – 01 (2018.02.09 11.56.05).csv	21.4	193.8	200.2	+3.32
T.2.2.2	T.2.2.2 – C02 – 01 (2018.02.09 11.57.52).csv	21.3	208.6	214.9	+3.04
T.2.2.3	T.2.2.3 – C02 – 01 (2018.02.09 12.00.23).csv	20.7	234.5	243.3	+3.76
T.2.2.4	T.2.2.4 – C02 – 01 (2018.02.09 12.02.29).csv	21.4	226.2	233.3	+3.14
T.2.3.1	T.2.3.1 – C02 – 01 (2018.02.09 09.44.07).csv	22.0	160.7	166.7	+3.78
T.2.3.2	T.2.3.2 – C02 – 01 (2018.02.09 10.12.57).csv	25.6	255.0	266.6	+4.54
T.2.3.3	T.2.3.3 – C02 – 01 (2018.02.09 10.18.13).csv	29.4	303.3	316.2	+4.25
T.2.3.4	T.2.3.4 – C02 – 01 (2018.02.09 10.23.07).csv	22.7	232.4	240.6	+3.53

Table 37: Cyclist **C.03** – summary of the results of tests using a round ring.

test	file	angular velocity variation [%]	IAVpwr [W]	AAVpwr [W]	power error [%]
T.1.1.1	T.1.1.1 – C03 – 01 (2018.02.15 03.46.22).csv	6.1	261.3	259.4	−0.71
T.1.1.2	T.1.1.2 – C03 – 01 (2018.02.15 03.48.03).csv	4.3	256.2	255.1	−0.43
T.1.1.3	T.1.1.3 – C03 – 01 (2018.02.15 03.50.03).csv	7.3	326.3	322.6	−1.15
T.1.1.4	T.1.1.4 – C03 – 01 (2018.02.15 03.52.03).csv	10.3	335.4	330.0	−1.59
T.1.2.1	T.1.2.1 – C03 – 01 (2018.02.15 03.57.01).csv	5.2	258.0	257.7	−0.12
T.1.2.2	T.1.2.2 – C03 – 01 (2018.02.15 03.58.58).csv	5.8	273.5	273.0	−0.18
T.1.2.3	T.1.2.3 – C03 – 01 (2018.02.15 04.00.38).csv	6.3	333.4	332.6	−0.24
T.1.2.4	T.1.2.4 – C03 – 01 (2018.02.15 04.03.04).csv	7.3	330.8	329.5	−0.39
T.1.3.1	T.1.3.1 – C03 – 01 (2018.02.15 02.45.51).csv	5.4	245.7	246.0	+0.11
T.1.3.2	T.1.3.2 – C03 – 01 (2018.02.15 03.05.54).csv	8.0	357.2	359.4	+0.62
T.1.3.3	T.1.3.3 – C03 – 01 (2018.02.15 03.15.11).csv	9.7	360.6	360.7	+0.03
T.1.3.4	T.1.3.4 – C03 – 01 (2018.02.15 03.20.22).csv	5.0	262.1	262.6	+0.20

Table 38: Cyclist **C.03** – summary of the results of tests using an oval ring

test	file	angular velocity variation [%]	IAVpwr [W]	AAVpwr [W]	power error [%]
T.2.1.1	T.2.1.1 – C03 – 01 (2018.02.15 04.21.03).csv	17.3	270.3	277.9	+2.80
T.2.1.2	T.2.1.2 – C03 – 01 (2018.02.15 04.24.02).csv	18.0	260.3	268.5	+3.17
T.2.1.3	T.2.1.3 – C03 – 01 (2018.02.15 04.25.44).csv	16.8	340.9	348.3	+2.18
T.2.1.4	T.2.1.4 – C03 – 01 (2018.02.15 04.29.55).csv	16.5	312.6	317.7	+1.62
T.2.2.1	T.2.2.1 – C03 – 01 (2018.02.15 04.09.36).csv	21.9	257.6	266.1	+3.30
T.2.2.2	T.2.2.2 – C03 – 01 (2018.02.15 04.11.04).csv	20.3	268.6	278.8	+3.79
T.2.2.3	T.2.2.3 – C03 – 01 (2018.02.15 04.13.10).csv	21.8	329.5	340.1	+3.22
T.2.2.4	T.2.2.4 – C03 – 01 (2018.02.15 04.15.27).csv	22.6	333.1	342.1	+2.69
T.2.3.1	T.2.3.1 – C03 – 01 (2018.02.15 01.57.39).csv	23.0	257.7	266.6	+3.46
T.2.3.2	T.2.3.2 – C03 – 01 (2018.02.15 02.12.10).csv	27.2	350.2	362.3	+3.46
T.2.3.3	T.2.3.3 – C03 – 01 (2018.02.15 02.23.30).csv	29.6	383.3	398.5	+3.96
T.2.3.4	T.2.3.4 – C03 – 01 (2018.02.15 02.28.33).csv	24.5	276.5	287.3	+3.88

Table 39: Cyclist **C.04** – summary of the results of tests using a round ring.

test	file	angular velocity variation [%]	IAVpwr [W]	AAVpwr [W]	power error [%]
T.1.1.1	T.1.1.1 – C04 – 01 (2018.02.16 03.54.31).csv	3.1	216.1	215.6	−0.23
T.1.1.2	T.1.1.2 – C04 – 01 (2018.02.16 03.56.33).csv	2.6	172.8	172.7	−0.06
T.1.1.3	T.1.1.3 – C04 – 01 (2018.02.16 03.58.53).csv	3.9	276.6	276.0	−0.21
T.1.1.4	T.1.1.4 – C04 – 01 (2018.02.16 04.01.28).csv	6.5	261.1	259.9	−0.47
T.1.2.1	T.1.2.1 – C04 – 01 (2018.02.16 04.06.48).csv	3.7	200.5	200.4	−0.04
T.1.2.2	T.1.2.2 – C04 – 01 (2018.02.16 04.09.10).csv	4.0	209.9	210.1	+0.07
T.1.2.3	T.1.2.3 – C04 – 01 (2018.02.16 04.11.35).csv	4.0	252.7	252.7	−0.01
T.1.2.4	T.1.2.4 – C04 – 01 (2018.02.16 04.13.47).csv	5.2	243.2	242.9	−0.13
T.1.3.1	T.1.3.1 – C04 – 01 (2018.02.16 02.55.38).csv	4.4	168.8	169.0	+0.15
T.1.3.2	T.1.3.2 – C04 – 01 (2018.02.16 03.11.41).csv	6.9	258.8	260.4	+0.63
T.1.3.3	T.1.3.3 – C04 – 01 (2018.02.16 03.17.11).csv	9.0	306.0	307.3	+0.41
T.1.3.4	T.1.3.4 – C04 – 01 (2018.02.16 03.22.57).csv	4.7	165.8	165.9	+0.06

Table 40: Cyclist **C.04** – summary of the results of tests using an oval ring.

test	file	angular velocity variation [%]	IAVpwr [W]	AAVpwr [W]	power error [%]
T.2.1.1	T.2.1.1 – C04 – 01 (2018.02.16 04.31.26).csv	19.9	213.5	218.8	+2.50
T.2.1.2	T.2.1.2 – C04 – 01 (2018.02.16 04.33.38).csv	21.0	195.3	200.0	+2.40
T.2.1.3	T.2.1.3 – C04 – 01 (2018.02.16 04.35.20).csv	19.5	291.4	298.0	+2.29
T.2.1.4	T.2.1.4 – C04 – 01 (2018.02.16 04.37.22).csv	18.3	278.4	284.6	+2.23
T.2.2.1	T.2.2.1 – C04 – 01 (2018.02.16 04.19.53).csv	22.7	202.6	208.4	+2.88
T.2.2.2	T.2.2.2 – C04 – 01 (2018.02.16 04.22.07).csv	22.8	214.5	220.6	+2.86
T.2.2.3	T.2.2.3 – C03 – 01 (2018.02.16 04.24.24).csv	22.9	258.2	265.4	+2.76
T.2.2.4	T.2.2.4 – C04 – 01 (2018.02.16 04.26.43).csv	22.2	247.3	253.9	+2.69
T.2.3.1	T.2.3.1 – C04 – 01 (2018.02.16 02.07.33).csv	23.8	180.2	187.3	+3.93
T.2.3.2	T.2.3.2 – C04 – 01 (2018.02.16 02.23.41).csv	27.5	275.0	287.1	+4.41
T.2.3.3	T.2.3.3 – C01 – 01 (2018.02.16 02.29.29).csv	26.5	308.5	318.0	+3.09
T.2.3.4	T.2.3.4 – C04 – 01 (2018.02.16 02.34.49).csv	23.7	159.7	165.6	+3.68

Table 41: Cyclist **C.05** – summary of the results of tests using a round ring.

test	file	angular velocity variation [%]	IAVpwr [W]	AAVpwr [W]	power error [%]
T.1.1.1	T.1.1.1 – C05 – 01 (2018.02.19 03.31.24).csv	5.6	234.8	233.7	−0.49
T.1.1.2	T.1.1.2 – C05 – 01 (2018.02.19 03.33.06).csv	6.1	222.6	221.1	−0.66
T.1.1.3	T.1.1.3 – C05 – 01 (2018.02.19 03.35.16).csv	6.2	262.7	261.2	−0.57
T.1.1.4	T.1.1.4 – C05 – 01 (2018.02.19 03.37.31).csv	7.6	234.1	232.6	−0.64
T.1.2.1	T.1.2.1 – C05 – 01 (2018.02.19 03.43.16).csv	5.2	224.2	223.7	−0.22
T.1.2.2	T.1.2.2 – C05 – 01 (2018.02.19 03.45.09).csv	7.9	250.1	248.8	−0.52
T.1.2.3	T.1.2.3 – C05 – 01 (2018.02.19 03.47.08).csv	5.2	274.1	273.6	−0.19
T.1.2.4	T.1.2.4 – C05 – 01 (2018.02.19 03.49.14).csv	6.5	272.8	271.9	−0.33
T.1.3.1	T.1.3.1 – C05 – 01 (2018.02.19 02.38.43).csv	10.1	178.8	178.8	−0.04
T.1.3.2	T.1.3.2 – C05 – 01 (2018.02.19 02.54.32).csv	7.9	259.5	260.3	+0.31
T.1.3.3	T.1.3.3 – C05 – 01 (2018.02.19 03.00.28).csv	11.4	292.2	293.5	+0.43
T.1.3.4	T.1.3.4 – C05 – 01 (2018.02.19 03.06.14).csv	11.6	179.9	180.1	+0.13

Table 42: Cyclist **C.05** – summary of the results of tests using an oval ring.

test	file	angular velocity variation [%]	IAVpwr [W]	AAVpwr [W]	power error [%]
T.2.1.1	T.2.1.1 – C05 – 01 (2018.02.19 04.08.29).csv	18.0	221.4	228.0	+2.98
T.2.1.2	T.2.1.2 – C05 – 01 (2018.02.19 04.10.12).csv	18.2	187.8	194.0	+3.30
T.2.1.3	T.2.1.3 – C05 – 01 (2018.02.19 04.12.56).csv	17.7	280.6	288.4	+2.77
T.2.1.4	T.2.1.4 – C05 – 01 (2018.02.19 04.15.42).csv	18.1	258.5	263.3	+1.85
T.2.2.1	T.2.2.1 – C05 – 01 (2018.02.19 03.55.25).csv	21.5	221.9	229.0	+3.20
T.2.2.2	T.2.2.2 – C05 – 01 (2018.02.19 03.57.13).csv	20.1	244.4	253.1	+3.56
T.2.2.3	T.2.2.3 – C05 – 01 (2018.02.19 04.00.10).csv	20.0	272.7	281.7	+3.30
T.2.2.4	T.2.2.4 – C05 – 01 (2018.02.19 04.02.24).csv	21.3	268.2	275.5	+2.72
T.2.3.1	T.2.3.1 – C05 – 01 (2018.02.19 01.46.54).csv	21.3	191.3	198.8	+3.95
T.2.3.2	T.2.3.2 – C05 – 01 (2018.02.19 02.09.44).csv	24.6	263.5	273.6	+3.87
T.2.3.3	T.2.3.3 – C05 – 01 (2018.02.19 02.15.59).csv	30.0	310.5	322.4	+3.84
T.2.3.4	T.2.3.4 – C05 – 01 (2018.02.19 02.21.44).csv	22.6	178.1	185.8	+4.29

Charts displaying force and angular velocity

The following charts show a typical pedal stroke for each type of test. The 5 cyclists are associated with different colors: C.01 – red, C.02 – green, C.03 – blue, C.04 – brown, C.05 – light blue.

It must be noted that starting angle 0° is not associated with a definite position of the crank arm.

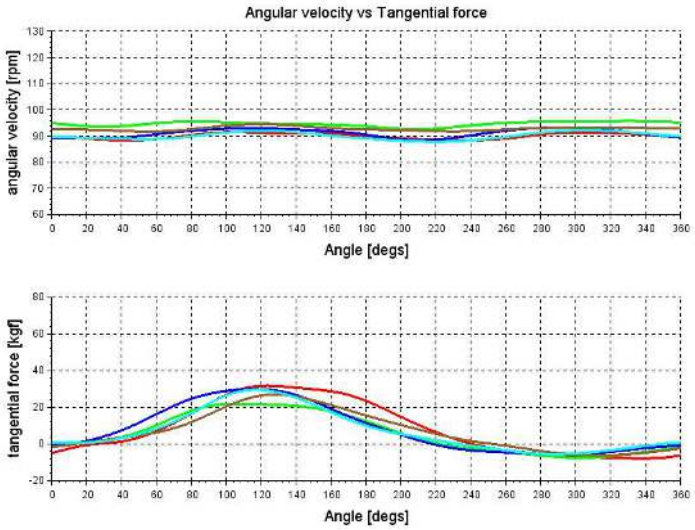

Fig. 4: **T.1.1.1 – A01**: round ring, Elite Qubo trainer, seated, FTP 70%, cadence 90 rpm – Example of single pedal revolution

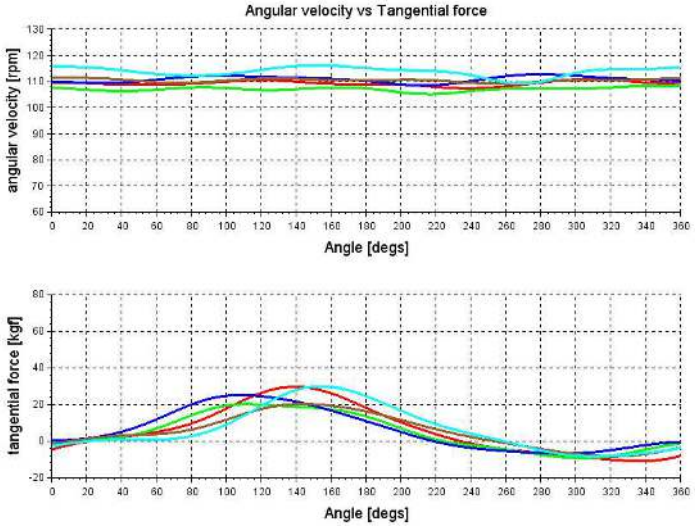

Fig. 5: **T.1.1.2 – A01**: round ring, Elite Qubo trainer, seated, FTP 70%, cadence 110 rpm – Example of single pedal revolution

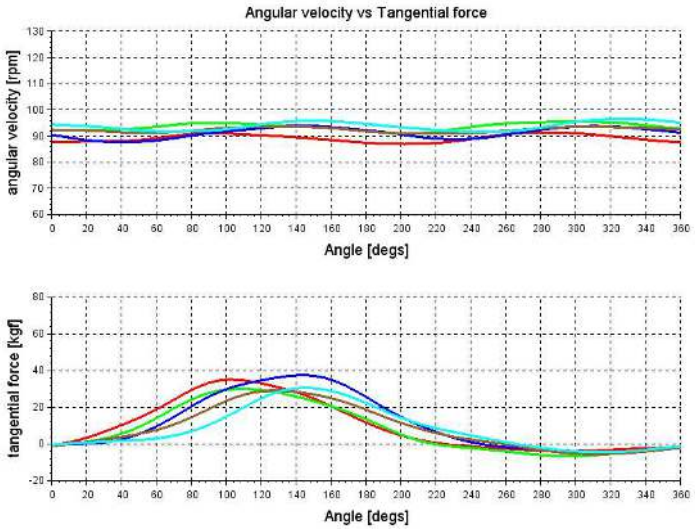

Fig. 6: **T.1.1.3 – A01**: round ring, Elite Qubo trainer, seated, FTP 95%, cadence 90 rpm – Example of single pedal revolution

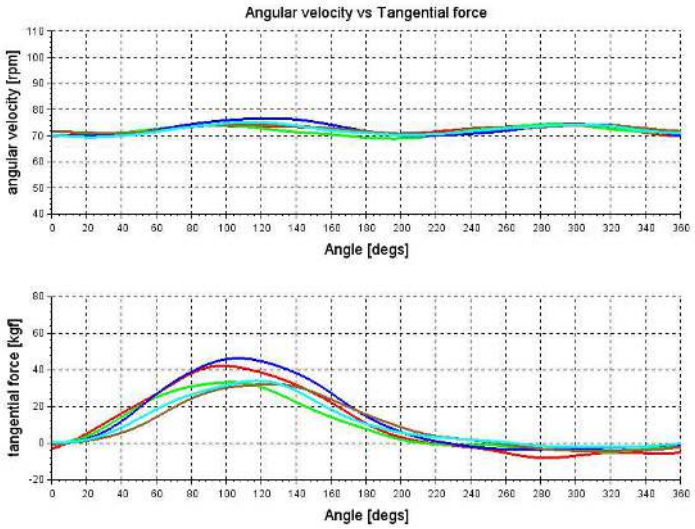

Fig. 7: **T.1.1.4 – A01**: round ring, Elite Qubo trainer, seated, FTP 95%, cadence 70 rpm – Example of single pedal revolution

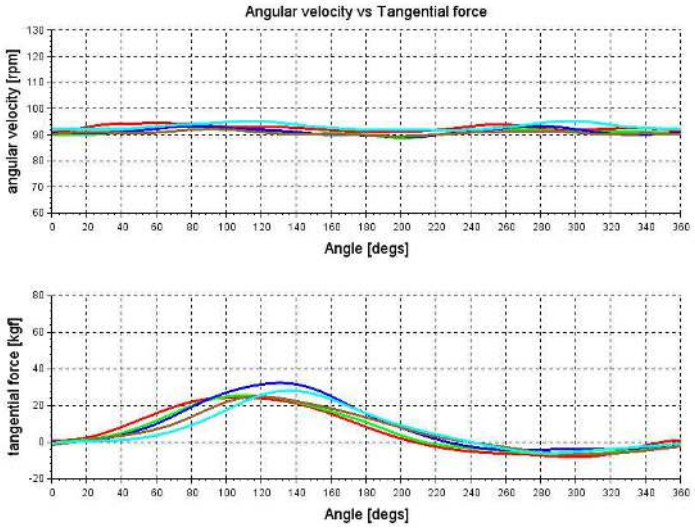

Fig. 8: **T.1.2.1 – A01**: round ring, Tacx NEO Smart trainer, seated, FTP 70%, cadence 90 rpm – Example of single pedal revolution

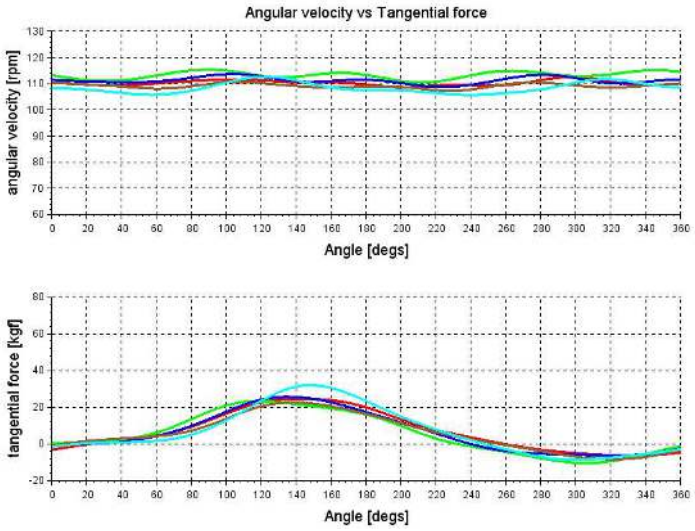

Fig. 9: **T.1.2.2 – A01**: round ring, Tacx NEO Smart trainer, seated, FTP 70%, cadence 110 rpm – Example of single pedal revolution

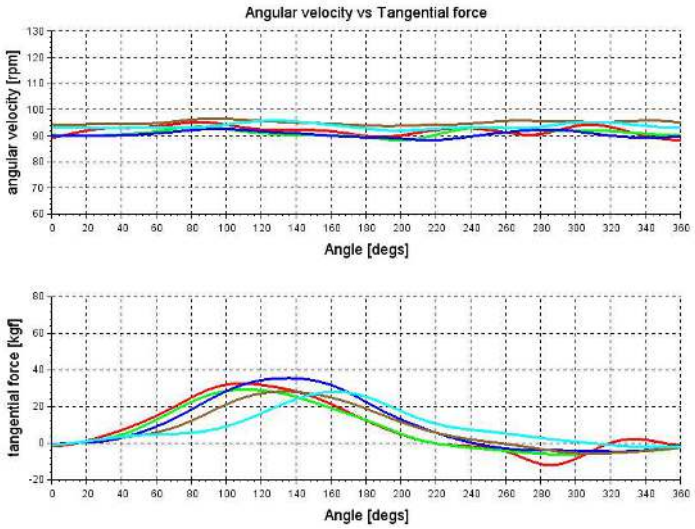

Fig. 10: **T.1.2.3 – A01**: round ring, Tacx NEO Smart trainer, seated, FTP 95%, cadence 90 rpm – Example of single pedal revolution

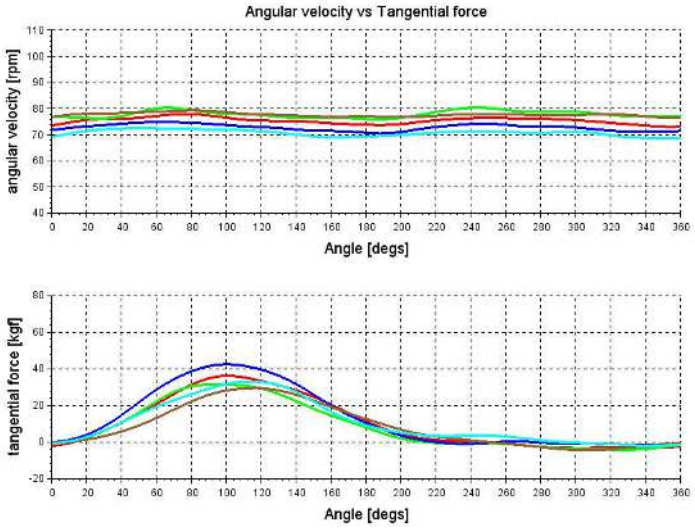

Fig. 11: **T.1.2.4 – A01**: round ring, Tacx NEO Smart trainer, seated, FTP 95%, cadence 70 rpm – Example of single pedal revolution

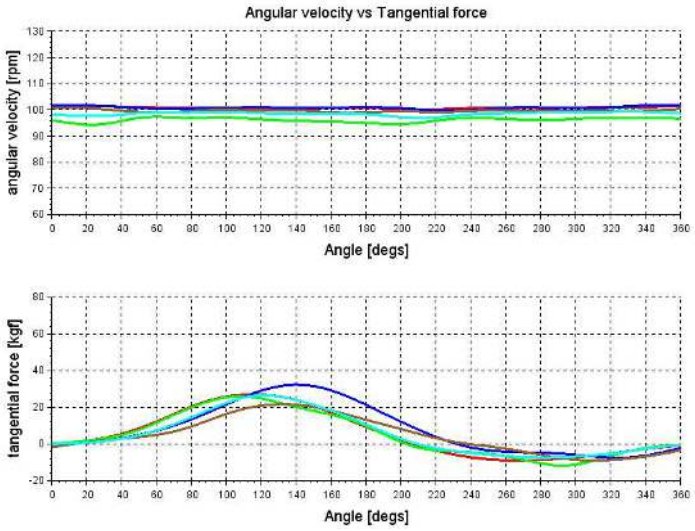

Fig. 12: **T.1.3.1 – A01**: round ring, on flat road, seated, cadence 100 rpm – Example of single pedal revolution

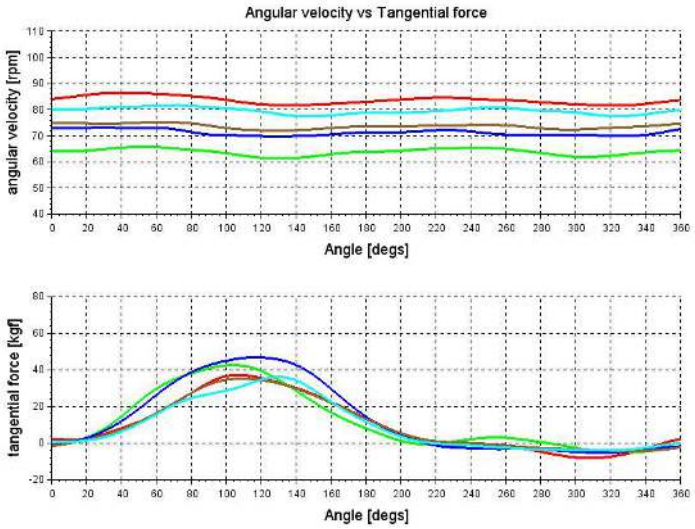

Fig. 13: **T.1.3.2 – A01**: round ring, on the road, 5% climb, seated – Example of single pedal revolution

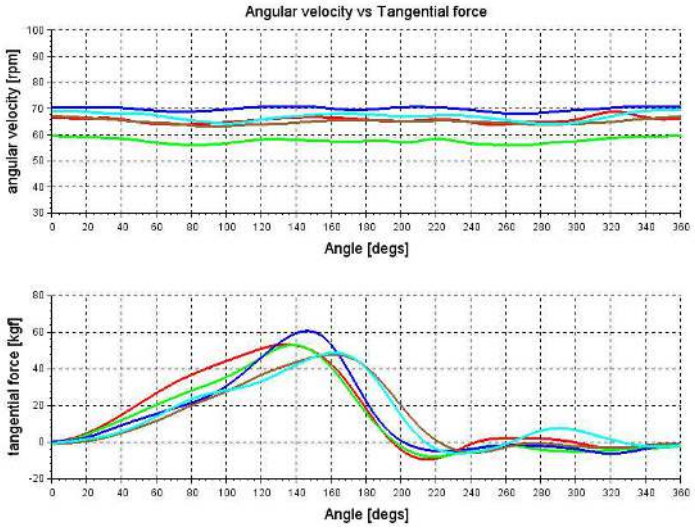

Fig. 14: **T.1.3.3 – A01**: round ring, on the road, 5% climb, standing – Example of single pedal revolution

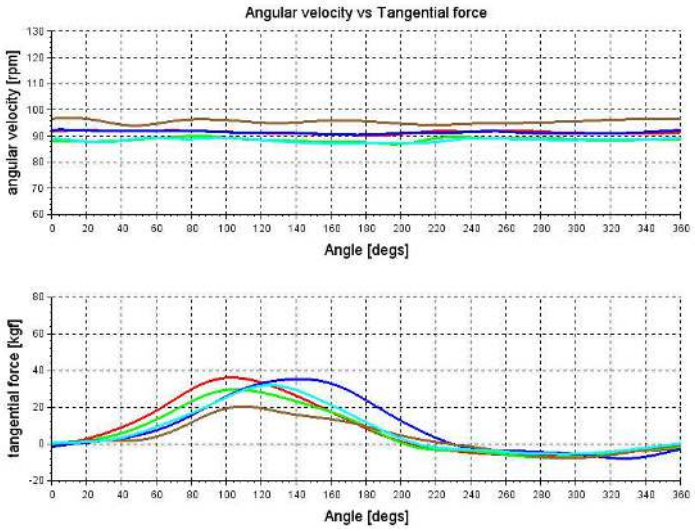

Fig. 15: **T.1.3.4 – A01**: round ring, on flat road, seated – Example of single pedal revolution

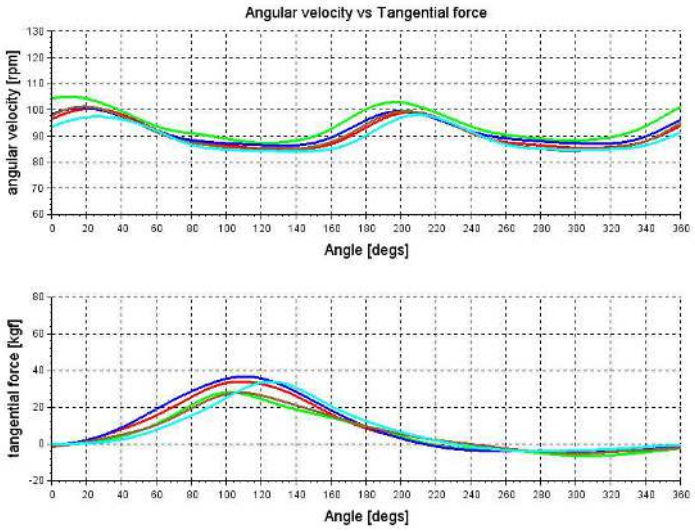

Fig. 16: **T.2.1.1 – A01**: oval ring, Elite Qubo trainer, seated, FTP 70%, cadence 90 rpm – Example of single pedal revolution

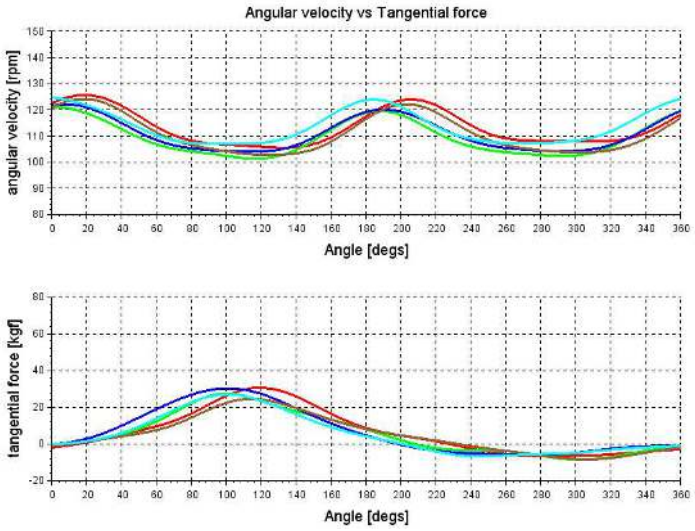

Fig. 17: **T.2.1.2 – A01**: oval ring, Elite Qubo trainer, seated, FTP 70%, cadence 110 rpm – Example of single pedal revolution

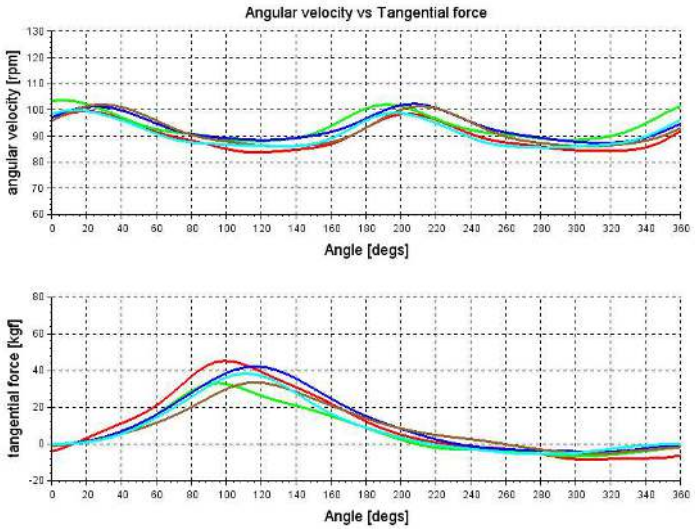

Fig. 18: **T.2.1.3 – A01**: oval ring, Elite Qubo trainer, seated, FTP 95%, cadence 110 rpm – Example of single pedal revolution

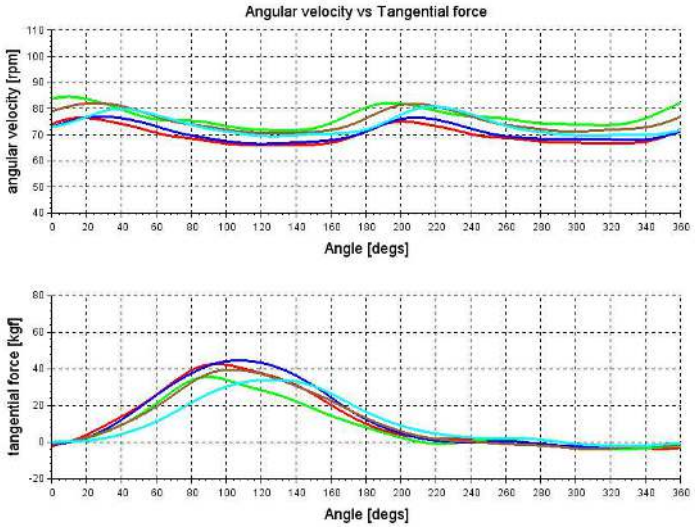

Fig. 19: **T.2.1.4 – A01**: oval ring, Elite Qubo trainer, seated, FTP 95%, cadence 70 rpm – Example of single pedal revolution

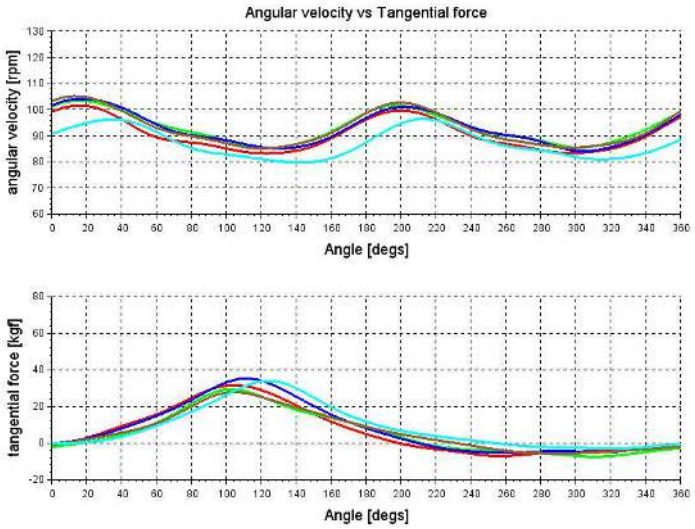

Fig. 20: **T.2.2.1 – A01**: oval ring, Tacx NEO Smart trainer, seated, FTP 70%, cadence 90 rpm – Example of single pedal revolution

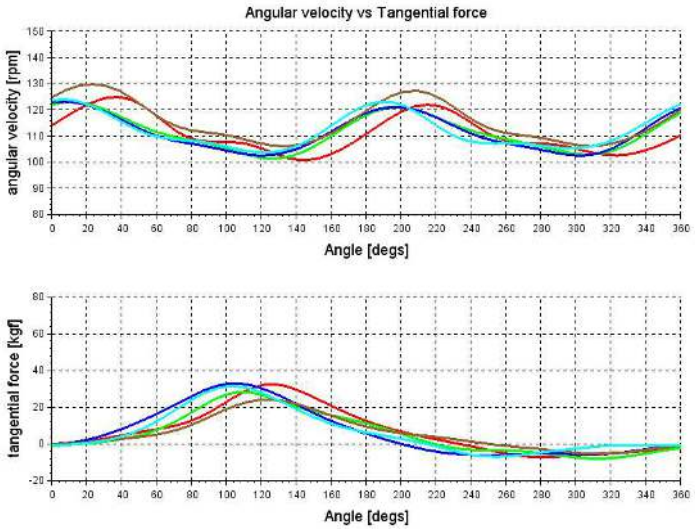

Fig. 21: **T.2.2.2 – A01**: oval ring, Tacx NEO Smart trainer, seated, FTP 70%, cadence 110 rpm – Example of single pedal revolution

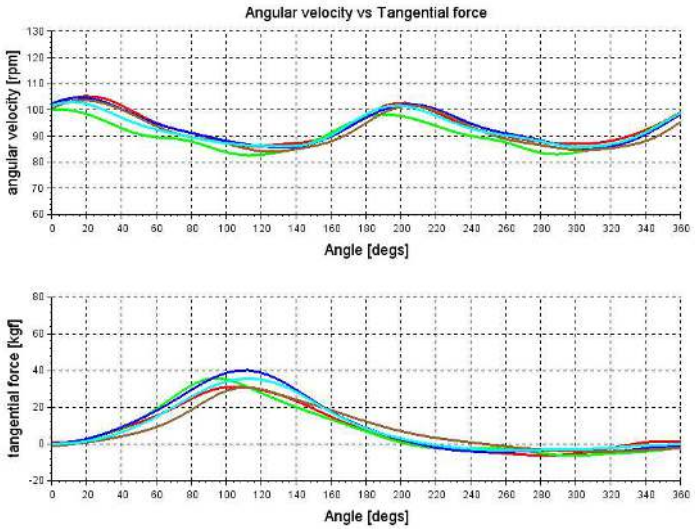

Fig. 22: **T.2.2.3 – A01**: oval ring, Tacx NEO Smart trainer, seated, FTP 95%, cadence 110 rpm – Example of single pedal revolution

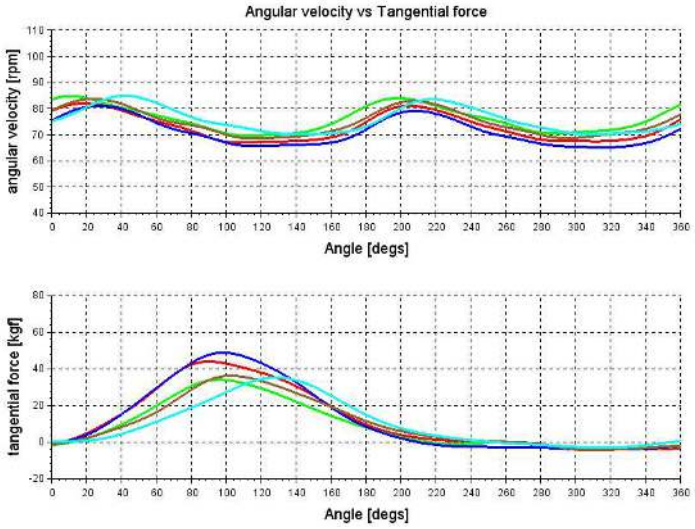

Fig. 23: **T.2.2.4 – A01**: oval ring, Tacx NEO Smart trainer, seated, FTP 95%, cadence 70 rpm – Example of single pedal revolution

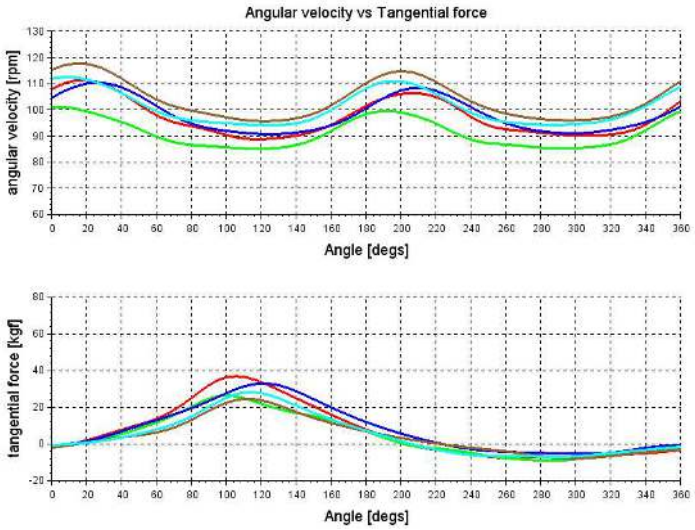

Fig. 24: **T.2.3.1 – A01**: oval ring, on the road, flat road, seated, cadence 100 rpm – Example of single pedal revolution

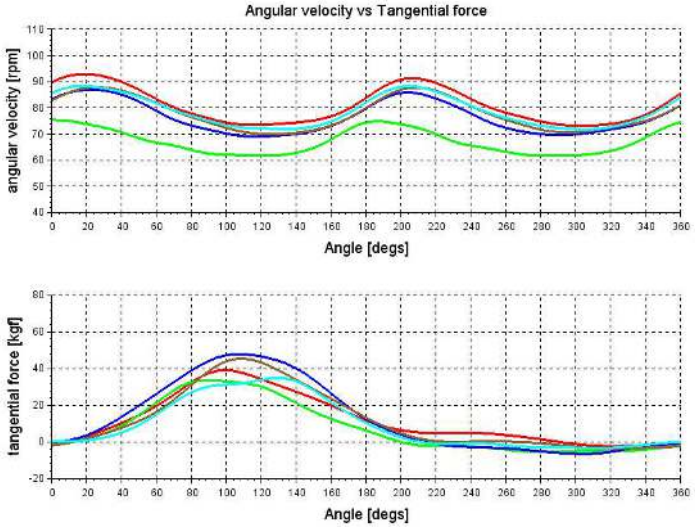

Fig. 25: **T.2.3.2 – A01**: oval ring, on the road, 5% climb, seated – Example of single pedal revolution

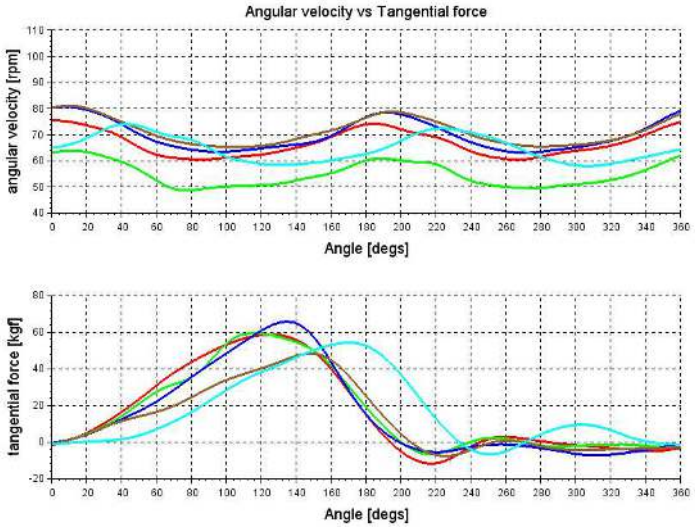

Fig. 26: **T.2.3.3 – A01**: oval ring, on the road, 5% climb, standing – Example of single pedal revolution

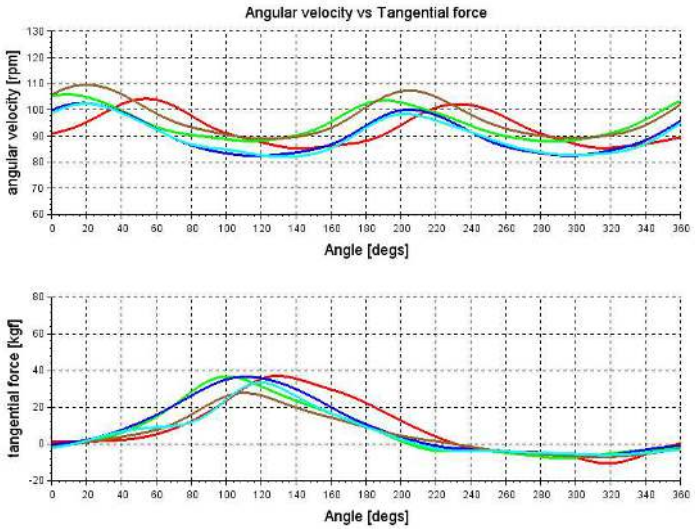

Fig. 27: **T.2.3.4 – A01**: oval ring, on the road, flat road, seated, cadence 90 rpm – Example of single pedal revolution

Appendix - Theory

Instantaneous power ***P(t)*** (in watts) at time ***t*** (in seconds) in a pedal stroke is given by:

$$\boldsymbol{P}(t)=\boldsymbol{F_T}(t)\cdot\boldsymbol{\omega}(t)\cdot\boldsymbol{b_C}$$

where:

- $\boldsymbol{F_T(t)}$ is the tangential force (in newtons),
- $\boldsymbol{\omega(t)}$ is the angular velocity (in rad/s) and
- $\boldsymbol{b_C}$ is the length (in meters) of the lever arm on which the force is applied.

To calculate the power of a pedal stroke $\boldsymbol{P_M}$ (in watts) the mean of instantaneous power ***P(t)*** is computed in a period ***T*** of crank arm rotation:

$$\boldsymbol{P_M}=\frac{1}{\boldsymbol{T}}\cdot\int_T\boldsymbol{P}(t)\cdot dt=\frac{1}{\boldsymbol{T}}\cdot\int_T\boldsymbol{F_T}(t)\cdot\boldsymbol{\omega}(t)\cdot\boldsymbol{b_C}\cdot dt$$

Both tangential force $\boldsymbol{F_T(t)}$, and angular velocity $\boldsymbol{\omega(t)}$ are not simple wave forms, but can be expressed as a Fourier series of sine waves (harmonics) extending by periodicity a single period.

$$\boldsymbol{F_T}(t)=\boldsymbol{F_T}(0)+\sum_{k=1}^{\infty}\boldsymbol{F_T}(k)\cdot\cos[\frac{2\pi kt}{\boldsymbol{T}}+\boldsymbol{\phi}(k)]$$

$$\boldsymbol{\omega}(t)=\boldsymbol{\omega}(0)+\sum_{n=1}^{\infty}\boldsymbol{\omega}(n)\cdot\cos[\frac{2\pi nt}{\boldsymbol{T}}+\boldsymbol{\theta}(n)]$$

where $\boldsymbol{F_T(0)}$ and $\boldsymbol{\omega(0)}$ are the average values of the quantities in period ***T***, $\boldsymbol{\varphi(k)}$ and $\boldsymbol{\theta(n)}$ are the phase shifts of the harmonics. Instantaneous power is therefore:

$$\begin{aligned}&\boldsymbol{P}(t)=\boldsymbol{F_T}(t)\cdot\boldsymbol{\omega}(t)\cdot\boldsymbol{b_C}\\&=\boldsymbol{b_C}\cdot[\boldsymbol{F_T}(0)+\sum_{k=1}^{\infty}\boldsymbol{F_T}(k)\cdot\cos[\frac{2\pi kt}{\boldsymbol{T}}+\boldsymbol{\phi}(k)]]\\&\cdot[\boldsymbol{\omega}(0)+\sum_{n=1}^{\infty}\boldsymbol{\omega}(n)\cdot\cos[\frac{2\pi nt}{\boldsymbol{T}}+\boldsymbol{\theta}(n)]]\end{aligned}$$

The products yield an expression made up of 4 terms:

$$\begin{aligned}&\boldsymbol{P}(t)=\\&\boldsymbol{b_C}\cdot\boldsymbol{F_T}(0)\cdot\boldsymbol{\omega}(0)+\\&\boldsymbol{b_C}\cdot\boldsymbol{F_T}(0)\cdot\sum_{n=1}^{\infty}\boldsymbol{\omega}(n)\cdot\cos[\frac{2\pi nt}{\boldsymbol{T}}+\boldsymbol{\theta}(n)]+\\&\boldsymbol{b_C}\cdot\boldsymbol{\omega}(0)\cdot\sum_{k=1}^{\infty}\boldsymbol{F_T}(k)\cdot\cos[\frac{2\pi kt}{\boldsymbol{T}}+\boldsymbol{\phi}(k)]+\\&\boldsymbol{b_C}\cdot\sum_{k=1}^{\infty}\sum_{n=1}^{\infty}\boldsymbol{F_T}(k)\cdot\boldsymbol{\omega}(n)\cdot\cos[\frac{2\pi kt}{\boldsymbol{T}}+\boldsymbol{\phi}(k)]\cdot\cos[\frac{2\pi nt}{\boldsymbol{T}}+\boldsymbol{\theta}(n)]\end{aligned}$$

Integrating the expression in a period ***T***, the first term gives:

$$\boldsymbol{P_{M1}}=\frac{\boldsymbol{b_C}}{\boldsymbol{T}}\cdot\int_T\boldsymbol{F_T}(0)\cdot\boldsymbol{\omega}(0)dt=\boldsymbol{b_C}\cdot\boldsymbol{F_T}(0)\cdot\boldsymbol{\omega}(0)$$

corresponding to the power obtained by multiplying the average values of the tangential force and angular velocity.

Integrating the first and second term into the period gives zero, ($\boldsymbol{P_{M2}}$ = $\boldsymbol{P_{M3}}$ = 0), since these are periodic terms of period ***T*** and therefore with a zero mean.

The fourth term can be rewritten as:

$$\begin{aligned}&\boldsymbol{P_{M4}}=\frac{\boldsymbol{b_C}}{\boldsymbol{T}}\cdot\int_T\sum_{k=1}^{\infty}\sum_{n=1}^{\infty}\frac{\boldsymbol{F_T}(k)\cdot\boldsymbol{\omega}(n)}{2}\cdot\\&\{\cos[\frac{2\pi(k+n)t}{\boldsymbol{T}}+\boldsymbol{\phi}(k)+\boldsymbol{\theta}(n)]+\cos[\frac{2\pi(k-n)t}{\boldsymbol{T}}+\boldsymbol{\phi}(k)-\boldsymbol{\theta}(n)]\}dt\end{aligned}$$

Proceeding to sum integration, one has:

$$\begin{aligned}&\boldsymbol{P_{M4}}=\frac{\boldsymbol{b_C}}{2\cdot\boldsymbol{T}}\cdot\sum_{k=1}^{\infty}\sum_{n=1}^{\infty}\boldsymbol{F_T}(k)\cdot\boldsymbol{\omega}(n)\cdot\\&\int_T\{\cos[\frac{2\pi(k+n)t}{\boldsymbol{T}}+\boldsymbol{\phi}(k)+\boldsymbol{\theta}(n)]+\cos[\frac{2\pi(k-n)t}{\boldsymbol{T}}+\boldsymbol{\phi}(k)-\boldsymbol{\theta}(n)]\}dt\end{aligned}$$

The first term in the integral still has a period that is a submultiple of ***T***, so its contribution is zero. The second term contributes with a value other than zero only when k = n (with k ≠ n, the period is a submultiple of ***T***), so one can proceed with:

$$\begin{aligned}&\boldsymbol{P_{M4}}=\frac{\boldsymbol{b_C}}{2\cdot\boldsymbol{T}}\cdot\sum_{k=1}^{\infty}\boldsymbol{F_T}(k)\cdot\boldsymbol{\omega}(k)\cdot\int_T\cos[\boldsymbol{\phi}(k)-\boldsymbol{\theta}(k)]dt\\&=\frac{\boldsymbol{b_C}}{2}\cdot\sum_{k=1}^{\infty}\boldsymbol{F_T}(k)\cdot\boldsymbol{\omega}(k)\cdot\cos[\boldsymbol{\phi}(k)-\boldsymbol{\theta}(k)]\end{aligned}$$

Considering the various contributions, the mean power of a pedal revolution is therefore:

$$\boldsymbol{P_M}=\boldsymbol{b_C}\cdot\boldsymbol{F_T}(0)\cdot\boldsymbol{\omega}(0)+\frac{\boldsymbol{b_C}}{2}\cdot\sum_{k=1}^{\infty}\boldsymbol{F_T}(k)\cdot\boldsymbol{\omega}(k)\cdot\cos[\boldsymbol{\phi}(k)-\boldsymbol{\theta}(k)]$$

Remarks

- In computing the mean power of a pedal stroke, a contribution is given by the product of the harmonics of the tangential force $\boldsymbol{F_T(k)}$ and angular velocity $\boldsymbol{\omega(k)}$ as long as they have same frequency (period).
- The contribution of these harmonics is in any case zero when they are shifted by 90°, i.e., $\boldsymbol{\varphi(k)}$ - $\boldsymbol{\theta(k)}$ = ±90°.
- Normally, angular velocity has a fundamental harmonic with a frequency double the tangential force, so the term $\boldsymbol{\omega(1)}$ is zero.
- Calculating the average power solely by multiplying the average values of the tangential force, $\boldsymbol{F_T(0)}$ and angular velocity $\boldsymbol{\omega(0)}$, i.e., considering only the first addend of the final expression, the contribution of the higher degree harmonics is neglected.
- It is not possible to establish a priori whether the harmonics can increase or decrease the result obtained from the average values.